

Clustered Saliency Prediction

Rezvan Sherkati

Electrical and Computer Engineering
McGill University
Montreal, Canada
rezvan.sherkati@mail.mcgill.ca

James J. Clark

Electrical and Computer Engineering
McGill University
Montreal, Canada
james.clark1@mcgill.ca

Abstract—We present a new method for image saliency prediction, Clustered Saliency Prediction. This method divides individuals into clusters based on their personal features and their known saliency maps, and generates a separate image saliency model for each cluster. We test our approach on a public dataset of personalized saliency maps, with varying importance weights for personal feature factors and observe the effects on the clusters. For each cluster, we use an image-to-image translation method, mainly Pix2Pix model, to convert universal saliency maps to saliency maps of that cluster. We try three state-of-the-art universal saliency prediction methods, DeepGaze II, ML-Net and SalGAN, and see their impact on the results. We show that our Clustered Saliency Prediction technique outperforms the state-of-the-art universal saliency prediction models. Also we demonstrate the effectiveness of our clustering method by comparing the results of Clustered Saliency Prediction using clusters obtained by Subject Similarity Clustering algorithm with two baseline methods. We propose an approach to assign new people to the most appropriate cluster, based on their personal features and any known saliency maps. In our experiments we see that this method of assigning new people to a cluster on average chooses the cluster that gives higher saliency scores.

**This manuscript is a pre-print currently under review at the Elsevier Journal Computer Vision and Image Understanding.*

I. INTRODUCTION

When humans are looking at a scene or are presented with an image, they might fixate on some points (i.e. fixation points) and spend more time looking at them. Knowing fixation points carries a lot of information, such as features of the image and the important events that might be happening in the image. It can also reflect on the personality traits of the subject. For this reason, the problem of analyzing and predicting fixation points in an image, i.e. saliency prediction, has been an important research problem for decades.

In the previous works in this area, visual saliency data have been collected by eyetrackers [1]. More recently with the growing need to collect large-scale data, researchers have used approaches such as gaze tracking using mouse clicks, [2], [3] and webcams [4]. A saliency map is often created from the fixation points by convolving them with a Gaussian kernel. The result is a gray-scale image or a heat map, where each pixel can be thought of as the probability of its corresponding pixel in the image to attract human attention.

One of the early works in the area of universal saliency prediction is the model by [5], where image features are combined into a topographical saliency map and then a dynamical neural network selects certain locations of this saliency map

and generates the final result. This work started an era of several works in this area and specially in the last decade with great improvements in the area of deep neural networks, there has been a lot of progress made in this subject [6].

Even though there have been much improvement in the area of saliency prediction and many efficient and reliable models have been presented, there are still many weak points to these models, and serious questions remain as to the applicability of them. One of the most important concerns is the fact that the fixation patterns and saliency maps differ across different individuals. There are many other factors other than image features that might affect one's fixation locations. It is undeniable that personal features, biases and personality traits have huge effects on individual attention patterns and saliency maps. For example in viewing a typical image, it is highly likely that there are many differences between the fixation points of a teenager and the ones of an elderly person. For this reason, it is essential to study saliency prediction from a personalized point of view, i.e. personalized saliency prediction.

The applications of saliency prediction and specifically personalized saliency prediction are numerous. Models developed for the purpose of personalized saliency prediction will help us explore the effects of personal features and traits and biases on gaze patterns and human attention. Thus it enables us to study human behavior more deeply and discover new perspectives on it. Also the developed models can be used for many different applications such as customer demand prediction in retail, targeted advertisement [7], [8], human-computer interaction [9], distraction analysis in images, patient diagnosis, virtual reality and augmented reality [10].

In this paper, in order to study saliency prediction from a more personalized perspective, we introduce a new approach called Clustered Saliency Prediction. We define this as the prediction of saliency maps for groups of similar individuals. We have developed methods to first, group individuals based on some personal features and their previous available saliency data (if there exists any). Then, considering this grouping or clustering of individuals, we can learn to predict the saliency map of individuals belonging to a specific group.

A major part of our approach for predicting saliency is to find an appropriate clustering of the subjects. Ideally each cluster should contain individuals that have a similar attention pattern when looking at an image. For clustering

of individuals, we propose the Subject Similarity Clustering method, which is a network-based algorithm which builds a network using personalized saliency maps of individuals and their personal features. Then we use the Louvain community detection algorithm on this network to find the clusters. The reason behind using a network structure is to take into account all the factors in relation to each other in a single entity. One important part of our research is to unravel the effect of different factors on clustering of individuals and how well different clustering settings perform in putting individuals with similar attention patterns in the same cluster.

After putting individuals in appropriate clusters, we will use an image-to-image translation (I2I) model for predicting saliency maps in each cluster. In more detail, we use the I2I model for translating universal saliency maps to the saliency maps in a specific cluster. We show that the performance in most of the evaluation metrics in clustered saliency prediction is higher than state-of-the-art universal saliency prediction methods. We will test our methods on multiple different settings of clustering and compare the performances to two baseline cases, first the case with no clustering (training I2I on all the individuals) and also to the case with random clustering (putting individuals randomly in 3 different groups). We show that in some settings of clustering, the performance is higher than the baseline cases, which proves the effectiveness of the Subject Similarity Clustering using a range of feature weights. We also propose a method to assign new people to the most appropriate cluster, using their personal features and any known saliency map of the person. We demonstrate this method's effectiveness in choosing the best cluster in a few scenarios by doing some experiments.

Methods in I2I problems can be highly applicable to the problem of predicting clustered saliency maps from universal saliency maps. The reason is that in I2I applications, a good amount of low-level information is shared between input and output and the network learns to transfer much of this information across input and output, and also transform the more subtle differences from input domain to output domain. This is very similar to the application of converting universal saliency maps to clustered saliency maps, since the clustered saliency maps have a lot of similarities with the universal saliency maps, and there are some smaller differences which are due to the variation in different individuals' patterns of attention. An appropriate I2I method will be able to detect this main similarities between these two domains and distinguish the differences as well.

There are multiple advantages to clustered saliency prediction over individually personalized saliency prediction. First, by aggregating the saliency maps of similar individuals in clusters, we omit the unimportant noises and will be able to catch the main themes in the saliency patterns. Another advantage is that by putting individuals in clusters, their privacy would be further preserved, since it will be more difficult to associate an output with a specific user.

In summary, our contributions in this paper are as below:

- Proposing a new clustering method, Subject Similarity

Clustering, using a network based structure and Louvain community detection algorithm.

- Using I2I methods to convert universal saliency predictions using state-of-the-art methods, to saliency maps of each cluster.
- Conducting experiments on a publicly available dataset containing personalized saliency maps, and proving the superiority of our results to state-of-the-art universal saliency prediction methods.
- Proving the effectiveness of our clustering method in improving prediction of saliency maps, by comparing the results with two baseline cases.
- Proposing a method to assign new people to their closest clusters, using their personal features and any of their available saliency maps.

In the next section, we will review related work. Following that we will introduce the dataset that we mainly use throughout the paper to perform experiments. Then we will describe the evaluation metrics that we used. Finally, we will present our methods and the results of the experiments.

II. RELATED WORK

A. Universal saliency prediction

Some of the first works in the area of saliency prediction are [5], [11], [12]. These early models mostly were based on extracting simple feature maps from the images. In [13], they have focused on extracting high-level image features such as faces, text elements, and cell phones and the extent to which they attract attention. These works are not deep learning based and focus on universal saliency prediction.

After reemerging of deep neural networks (DNN), there have been many improvements in saliency prediction models. Some of the first DNN based works on saliency prediction are eDN model [14] and DeepGaze I [15]. In DeepGaze I, they have shown that deep convolutional networks that have been trained on computer vision tasks such as object detection, boost saliency prediction. In [16], authors introduce DeepGaze II model for universal saliency prediction that uses transfer learning from the VGG-19 network to achieve a good performance.

In [17], they take advantage of transfer learning for saliency prediction to solve the problem of data shortage. They try to address the large gap between human behavior and traditional saliency prediction models. They argue that this gap is due to limited capability of traditional models in predicting eye fixations with strong semantic content. For this, they use DNNs that are pretrained for object recognition, more specifically they use AlexNet, [18], VGG-16, [19] and GoogLeNet, [20]. They fine-tune the DNNs with an objective function based on the saliency evaluation metrics, and integrate information at different image scales (fine and coarse).

ML-Net is a deep-learning based architecture proposed in [21] for predicting universal saliency maps. This model uses multi-level features extracted from a CNN and it is end-to-end trainable.

In [22], they propose a model called DeepFix, which is a fully convolutional neural network. This model uses 5 convolution blocks whose weights initialized from the VGG-16 net. Since fully convolutional networks are location invariant, they can't learn location specific patterns such as the centre-bias. In order to address this, they utilize Location Biased Convolutional filters (LBC), which enables the deep network to learn location dependent patterns.

The model SalGAN [23], takes advantage of Generative Adversarial Networks (GAN), which consists of a VGG-16 based encoder-decoder model as the generator, and a discriminator, which tries to distinguishing between the real saliency maps and those generated by SalGAN.

The work in [24] proposed a model Deep Visual Attention (DVA) that works in an encoder-decoder architecture, where the decoder performs upsampling with trainable multi-channel kernels. The supervision is directly fed into hidden layers, encouraging the model to learn robust features and generate multi-scale saliency estimates. DVA model learns to combine multi-level saliency information from different layers with various receptive field sizes.

The model Attentional Push proposed in [25], combines standard saliency models, which generally concentrate on analyzing image regions for their power to attract attention, with Attentional Push cues, which they have limited in this work to gaze location of the scene actors. They have presented an attention modeling scheme, which learns to follow the gaze location of the scene actors and augments saliency models with Attentional Push.

There are several other works in this area. Some of these are [21], [26]–[34].

Also there has been some works done in the area of saliency prediction in videos. Some example of these works are [35]–[43].

B. Personalized saliency prediction

Some work has been done to address the problem of Personalization of Saliency Detection. The number of these works is low, however, as compared to the large literature on universal saliency prediction methods.

In [44], authors have produced a dataset of personalized saliency maps (PSMs), although this dataset has been modified and more correct explanation of the dataset are in the paper [45]. This dataset is described in more detail in Section III-A, since we are also using this dataset for training and testing our models. In [44] they model PSM based on universal saliency map (USM) shared by different participants and adopt a multitask CNN framework to estimate the discrepancy between PSM and USM.

In [45], which is an extended version of [44], similarly they decompose a PSM into a USM predictable by previous saliency detection models and a new discrepancy map across users that characterizes personalized saliency. Then they present a new solution in addition to their previous work towards predicting such discrepancy maps, which is an extended CNN with Person-specific Information Encoded

Filters (CNN-PIEF). They use person-specific information to generate filters and convolve these Person-specific Information Encoded Filters (PIEF) with the input feature maps, and these PIEF function as switches to determine which areas interest different observers.

The work by [46], proposed a derivative of the GAN network, which is adapted from the Conditional GAN and StackGAN architectures and is able to generate personalized saliency predictions. This augmented network contains a generator, which is combined with a discriminator. The discriminator's task is to distinguish fake saliency maps from real ones. The generator will later sense the answer backpropagated from the discriminator and become better at generating appropriate saliency maps. This model takes image stimuli and specific information about the observer as the input.

In [47], the authors develop Personalized Attention Network (PANet). PANet contains two streams of convolutional neural networks (CNNs) that share common feature extraction layers. One stream is for predicting the general saliency information, and the other one is for fitting user preference upon the information from detection layers. They share common image features that extracted by VGG-16 without its final classification layers as well as the convolutional layers in the detection part.

In [48] is proposed a framework called Personalized Visual Saliency (PVS), which is based on robust multi-task learning (RMTL) and incorporates individuality. The task of attention prediction is transformed into multiple regression models that are learned simultaneously. Both simple low-level features designed by prior knowledge and complex deep features extracted from pretrained CNNs are incorporated into the framework as input features. For deep features they extract certain layers from two pretrained deep models, VGG16 and GoogLeNet.

The paper [49] looks at individual differences in the tendency to fixate on different types of objects embedded in natural scenes. The work investigated the fixation behavior of more than 100 human adults freely viewing 700 complex scenes, containing thousands of semantically annotated objects. They observed that fixation tendencies for faces, text, food, touched, and moving objects varied among individuals and these differences were present from the first eye movement after image onset and highly consistent across images and time. This suggests individual gaze behavior is organized along semantic dimensions of biological significance. Following this work, in [50], authors tried to replicating these individual differences, and testing whether they can be estimated using a shorter test than the previous work. They showed that these differences can be estimated using about 40 to 100 images (depending on the tested dimension). Additional analyses revealed that only the first 2 seconds of viewing duration seem to be informative regarding these differences. Taken together, their findings suggest that reliable individual differences in semantic salience can be estimated with a test that in total takes less than 2 minutes of viewing.

One of the main limitations in personalized saliency predic-

tion is the lack of large saliency datasets for each individual. In [51], the authors proposed few-shot personalized saliency prediction using a small amount of training data based on adaptive image selection (AIS) considering object and visual attention. First they construct and train a multi-task CNN from the PSM dataset for predicting PSMs of individuals included in the PSM dataset. For predicting a PSM for the new target person, he/she needs to view several images to search for similar persons. Before this procedure, some images should be selected from the PSM dataset for calculating person similarities between the target person and those included in the PSM dataset. The images that are selected are important and if we have higher diversity of images and high variance of PSMs the results are more reliable. So in order to have a robust PSM prediction with reduction in the number of selected images, an adaptive image selection (AIS) scheme with the mentioned criteria is necessary. Next, the person similarity is calculated by using selected images included in the PSM dataset. These images are chosen by AIS focusing on the diversity of images and the variance of PSMs. For guaranteeing the high diversity of the selected images, AIS focuses on the kinds of objects included in the training images in the PSM dataset by using a deep learning-based object detection method. Then, objects that have high variances of PSMs are detected, and then images including such objects can adaptively be selected. Finally, FPSP of a target image for the new target person is realized on the basis of the person similarity and PSMs predicted by the multi-task CNN trained for the persons in the PSM dataset.

In a more recent work in [52], the proposed model is composed of universal saliency prediction module and personalized gaze probability prediction module and then result of these two modules are integrated to generate a final saliency map. The universal saliency prediction CNN is composed of encoder and decoder networks, with reference to the network structure of SegNet, [53]. This model has a number of advantages such as fewer parameters due to the absence of fully connected layers and the possibility of input layers with arbitrary size. For personalized saliency prediction module, information about objects that attracts attention of viewers presented with an image is learned by a neural network using the softmax function in its output layer. Then the learning results and object classification results for each pixel are used to generate a mask for attention trends. In the end the results of two modules are merged together to make the saliency prediction that incorporates viewer-dependent eye movements.

III. METHODS

In this section, we will describe our approaches and the experiments that we have conducted. First we will describe the dataset and briefly talk about some evaluation metrics. Next, we describe our method for clustering individuals into groups. Then we will talk about the universal saliency prediction methods that we used and image-to-image translation methods for translating universal saliency maps into the clusters' saliency maps.

A. Dataset used in experiments

In order to test our approaches, we used the dataset collected in [45]. This dataset is suitable for the nature of our research, since it contains personalized saliency maps for all subjects. Now we describe this dataset in more detail. The dataset consists of 1600 images with multiple semantic annotations, which were observed by 30 student participants (14 males, 16 females, aged between 20 and 25). Among 1600 images in this dataset, 1100 images are chosen from existing saliency detection datasets including SALICON, [2], ImageNet, [54], iSUN, [55], OSIE, [56], PASCAL-S, [57], 125 images are captured by the authors of the paper [45], and 375 images are gathered from the Internet.

In order to guarantee the accuracy of each individual's fixation map and to eliminate outliers, each image was viewed four times by each observer. The four saliency maps of the same picture observed by the same individual are then combined, and the result is used as the observer's ground truth for the personalized saliency maps (PSM) dataset. To obtain a continuous saliency map of an image from the raw data of eye tracker, the fixation locations are blurred via convolution with Gaussian functions.

The dataset also includes a survey to collect each observer's personal information. Specifically, the following information is collected - the observer's gender (1D), the preference to objects falling into the fashion category (ring, necklace, bracelet, earring, etc., 11D), the preference/disgust to colors (red, yellow, green, cyan, blue, purple, white, black, 16D), the preference to different sports (football, basketball, badminton, tabletennis, etc., 11D), and the preference to objects falling into other categories (IT, plant, texts, food, 4D). In Table I is a list of all the features in each category. Subjects responded to each feature with 0 or 1, which for the Gender category determines their gender and for other categories, their preferences to the corresponding feature. we used a one-hot encoding method to encode each subject's personal information. This encoded information for each subject is a 43-Dimensional vector. The personal information survey is conducted after the eye tracking, so it doesn't create biases when subjects are looking at the images. We will refer to this dataset in other sections as *PSM dataset*.

B. Evaluation metrics

Given a ground truth of fixation points, a saliency metric is a function that takes the predicted saliency as input and outputs a number, which evaluates the accuracy of this prediction. For a complete review of many saliency evaluation metrics, their comparison, and under which circumstances each should be used, you can see the works by [58] and [59].

For evaluating the performance of our saliency prediction method and compare it with other methods, we use AUC-Judd, CC, SIM and NSS metrics.

1) *Area under ROC Curve (AUC)*: A Receiver Operating Characteristic curve, or ROC curve, is a graphical representation of a binary classifier's diagnostic ability as its discrimination threshold is varied. The ROC curve is constructed

| Category | Features |
|----------|--|
| Gender | Sex |
| Fashion | Fashion, Ring, Necklace, Bracelet, Earring, Hairpin, Watch, Glasses, Tie, Belt, Kneelet |
| Color | Red (like), Yellow (like), Green (like), Cyan (like), Blue (like), Purple (like), White (like), Black (like), Red (dislike), Yellow (dislike), Green (dislike), Cyan (dislike), Blue (dislike), Purple (dislike), White (dislike), Black (dislike) |
| Sport | Auto, Sport, Football, Basketball, Badminton, Tabletennis, Tennis, Volleyball, Baseball, Billiards, Chess |
| Other | IT, Plant, Reading, Eat |

TABLE I: Detailed list of all features included in each category. Viewers should have assigned 0 or 1 to each feature.

by plotting the true positive rate (TP rate) versus the false positive rate (FP rate) at various threshold settings. Saliency prediction problems can be considered as a classification problems where each pixel can be classified as fixated or not. The Area Under the Curve (AUC) is a measure of a classifier’s ability to distinguish between classes and is used to summarise the ROC curve. AUC is the most common metric used for evaluating saliency maps. True and false positives are calculated differently in different AUC implementations.

One of the variations of AUC is AUC-Judd, [1]. In AUC-Judd, the TP rate for a given threshold is the ratio of true positives to total number of fixations, where true positives are saliency map values above threshold at fixated pixels. The FP rate is the ratio of false positives to the total number of saliency map pixels at a given threshold, where false positives are saliency map values above the threshold at unfixed pixels.

2) *Normalized Scanpath Saliency (NSS)*: Normalized Scanpath Saliency (NSS) was introduced by [60], computed as the average normalized saliency at fixated locations in the ground truth. Positive NSS indicates correspondence between saliency map and ground truth with a probability above chance, and negative NSS indicates anti-correspondence of the maps. Even in the presence of many low-valued false positives, a saliency model with high-valued predictions at fixated locations would receive a high AUC score. One of the advantages of NSS over AUC is that all false positives contribute to lowering the normalised saliency value at each fixation location, lowering the overall NSS score.

3) *Pearson’s Correlation Coefficient (CC)*: The Pearson’s Correlation Coefficient (CC), which is also called linear correlation coefficient, is a statistical method used in the science to determine the degree to which two variables are correlated or dependent on one another. CC can be used to measure the linear relationship between saliency map and ground truth fixation maps, by considering them as random variables. CC is symmetric and penalizes false positives and negatives equally

and is invariant to linear transformations. In the analysis where distinction of penalties between false positive and false negatives is required, other metrics may be more useful.

4) *Similarity (SIM)*: This metric measures the similarity between two distributions that are viewed as histograms. This metric is popular in the context of saliency detection, since it can compare two saliency maps. To obtain SIM between two saliency maps, after normalizing the maps, we obtain the sum of minimum values at each pixel. $SIM = 0$ indicates that there are no similarity between two saliency maps and $SIM = 1$ indicates the distributions are the same. SIM penalizes the predictions that do not consider all the ground truth density.

C. Clustering

Here we have focused on creating a network structure based on individuals’ information and then clustering individuals based on the information in the network. For clustering the individuals into groups, we created a weighted complex network of the 30 subjects in this dataset using images seen by the individuals and their personal features. Then we used a community detection method [61] on this weighted network, called the Louvain algorithm [62], for dividing the individuals into groups. We call this clustering algorithm *Subject Similarity Clustering*. Now, we will describe the Subject Similarity Clustering algorithm in detail.

First we initiate a network called G with 30 nodes, each corresponding to one subject. Then we randomly sample 100 images from all the images and for each image I , we get all 30 of the saliency maps of 30 subjects for I and cluster these saliency maps into K clusters, based on their pixel-wise similarity, using the K-Means algorithm. Then, considering this clustering of saliency maps, if two subjects fall in the same cluster, in G we either add an edge with weight 1 between them, or increase the weight of the already existing edge by 1 (depending on if they are already connected or not). We repeat the above procedure for all the 100 sampled images. The reason for sampling 100 images instead of using all the images is to not make the network very dense, so the clustering algorithm can distinguish different clusters in the network.

After this, we incorporate the personal features of subjects in the network. As mentioned before, we have some information about each subject, such as their preferences in different colors, objects related to fashion, sport and etc. In order to process this information, for each subject, we make a vector of the aggregate of their information, i.e. the personal feature vector. Then using the K-Means clustering algorithm, we cluster personal feature vectors of all the subjects, into K clusters. Now in this clustering, if two subjects fall into the same cluster, depending whether they are already connected or not, in G we either add an edge with weight W between them, or increase the weight of the edge already existing between them by W . In fact, W is proportional to the importance and impact we want to give to the personal features in the network. As we will see in section IV, we will vary W and set of personal features across different clustering settings to see their effect on the clustering.

Using this algorithm for constructing the network, we get a weighted network in which the weight of the link between two subjects is an indicator of how similar their personal features and their attention in viewing different images are. For ease of reference in the future, we call the obtained network *Subject Similarity Network*.

For clustering the subjects, we chose the Louvain algorithm, since this algorithm works well with weighted network. The Louvain algorithm is a heuristic algorithm which aims at maximizing modularity in the process of detection of communities. One of the nice features of this algorithm is that it does not require number of communities or size of them, before execution. The Louvain algorithm is comprised of two phases, Modularity Optimization and Community Aggregation. These two phases are executed one after each other, until no improvement in maximum modularity is obtained. By applying the Louvain community detection algorithm, our Subject Similarity Clustering algorithm is completed and we have the clusters.

In Table II, you can see the parameters for different settings that we used in Subject Similarity Clustering to obtain clusters, for performing part of our experiments in Section IV-B. In this table, W is the weight of features vector (one-hot encoded personal information) in each setting. Also $K = 6$ is the number of clusters given as input to K-Means algorithm, for clustering all individuals' saliency maps for each image, in the process of creating Saliency Similarity Network, as described in more detail earlier.

In Fig. 1, you can see the visualization of constructed Subject Similarity Networks for the mentioned settings in Table II and the detected communities (clusters) by the Louvain algorithm. In each network, node numbers are the subject ID in the PSM dataset. Also, in each setting, nodes of same color belong to the same community. We have highlighted the highest weighted edge in each network by red. Note that these networks are weighted, although the weights of the edges are not shown in this figure for clarity.

For each setting of clustering and each cluster, for all the feature categories, the average of features vectors similarities between all the pairs of individuals in that cluster can be seen in Table III. In this table you can also find the average and median of similarities for all the pairs of individuals in the dataset.

D. Universal saliency prediction

For universal saliency prediction, we evaluated some of the state-of-the-art methods, such as DeepGaze II [16], ML-Net [21] and SalGAN [23]. As we will see in section III-E, we use the universal saliency maps obtained by these methods as the source images in training image-to-image translation models.

E. Image-to-image translation

As mentioned earlier, in order to convert the images from the universal domain to the clustered domains, for each cluster, we use an image-to-image translation (I2I) model. The goal of I2I is to learn a mapping to convert an input image x_A from a

| Setting | W | Number of resulting clusters |
|-----------|-----|------------------------------|
| Setting 0 | 0 | 3 |
| Setting 1 | 0.1 | 3 |
| Setting 2 | 0.5 | 3 |
| Setting 3 | 1 | 3 |
| Setting 4 | 4 | 3 |
| Setting 5 | 20 | 3 |
| Setting 6 | 100 | 4 |

TABLE II: Parameters for all clustering settings used in Section IV-B of experiments. W is the weight of personal features in each setting. In each of these settings, all of the features were used for clustering. For all these settings, $K = 6$, where K is the number of clusters given as input to the K-Means algorithm for clustering all individuals' saliency maps for each image, in the process of creating the Saliency Similarity Network.

source domain A to a target domain B , such that the intrinsic source content is preserved and the extrinsic target style is transferred. To do this, we need to train a mapping $G_{A \rightarrow B}$, that given image $x_A \in A$, generates an image $x_{AB} \in B$, which cannot be distinguished from images in B .

The problems in this area are divided into two categories, two-domain I2I tasks, where images are translated between only two domains, and multi-domain tasks, where images are translated between multiple domains. These models can be further divided into supervised, unsupervised and semi-supervised and few-shot methods.

For our application, we propose to use a two-domain I2I model. As we mentioned before, for a given clustering of individuals, we train an I2I model for each cluster, in order to convert universal saliency maps to saliency maps for that cluster. In Fig. 2 you can see a general overview of the process of converting universal saliency to clustered saliency maps using an I2I model. We will describe the approach for defining source and target sets for the I2I model in Section III-F.

Next, we give a brief overview of two of the I2I approaches that we have tried.

1) *UNsupervised Image-to-image Translation (UNIT) approach*: In [63], the authors propose the UNIT framework, which is based on generative adversarial networks (GANs) and variational autoencoders (VAEs). This is a two-domain unsupervised I2I model which assumes that a pair of corresponding images in different domains can be mapped to the same latent code in a shared latent space. They demonstrate that the cycle-consistency constraint is implied by the shared-latent space constraint.

2) *Pix2Pix approach*: The GAN based I2I model, Pix2Pix was proposed in [64]. This method uses a GAN in a conditional setting, where they condition on an input image and generate a corresponding output image. This is a two-domain supervised I2I model, where for training, images should be paired. In this model, the Conditional GAN (cGAN) objective is mixed with an L1 distance loss. The objective of the

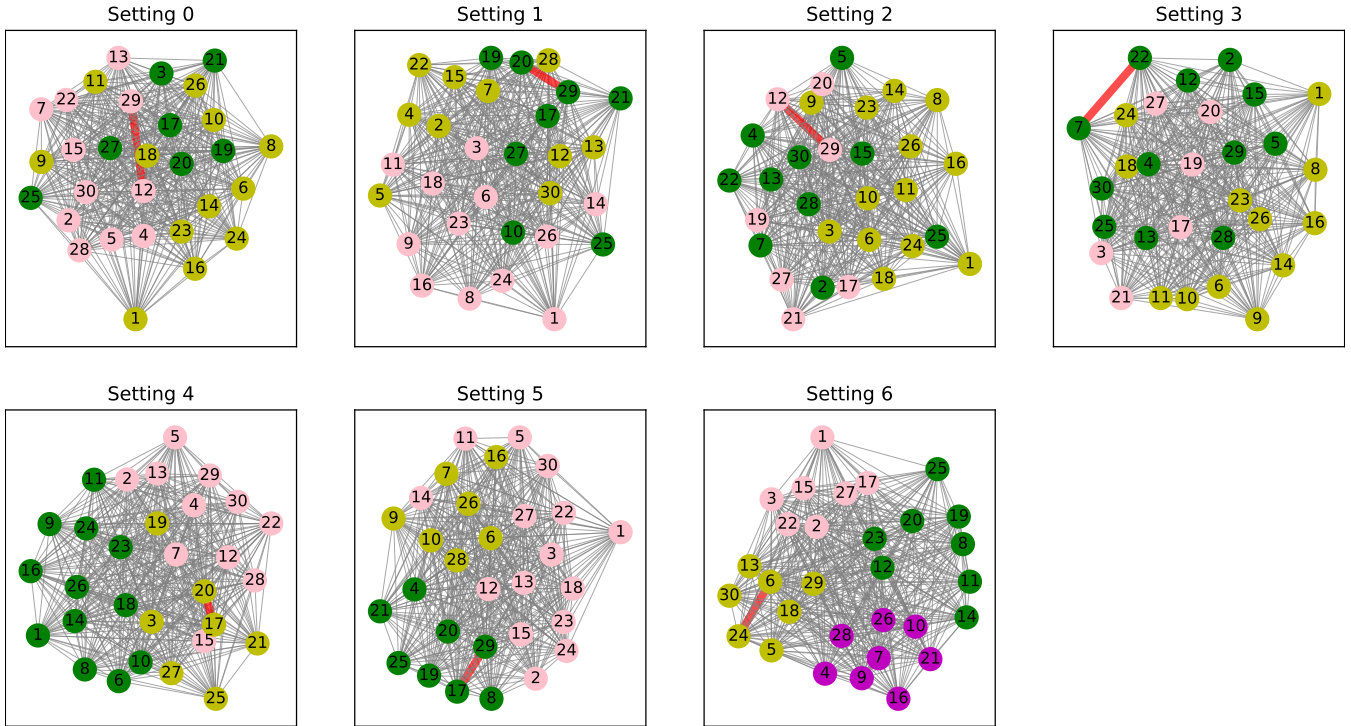


Fig. 1: Subject Similarity Networks for experimented clustering Settings 0 to 6, mentioned in Table II and used in Section IV-B of experiments. In each network, the edge with highest weight is depicted as red.

discriminator remains the same as cGAN. The generator, in addition to fooling the discriminator, needs to generate outputs that are near the ground truth in an L1 distance aspect. Thus, the objective of the Pix2Pix model is as below:

$$G^* = \arg \min_G \max_D \mathcal{L}_{cGAN}(G, D) + \lambda \mathcal{L}_{L1}(G) \quad (1)$$

In this network, generator and discriminator use modules of the form convolution-BatchNorm-ReLU. The generator has a U-Net [65] architecture with skip connections, which help to transfer across the network a great deal of low-level information that is shared between input and output. Also they introduce a discriminator architecture, PatchGAN, which only penalises structure on a patch-by-patch basis.

In order to test this model, we train Pix2Pix for each cluster, for many different clustering settings. We use the same hyperparameters as the original paper for training Pix2Pix, except for number of epochs, which will vary in some cases. In the next section, we will describe the source and target datasets for training I2I models.

F. Training approach for image-to-image translation models

For training the I2I model for each cluster, we set the source and target sets as following.

Suppose that after clustering individuals in Subject Similarity Network, we have n clusters C_1, C_2, \dots, C_n . Assume that in PSM dataset we have personalized saliency maps for a set of images I . We train an I2I model for each cluster C_i , where the source images are the universal saliency maps for images in I , as described in Section III-D. We denote the universal saliency

maps of an image x obtained using method M by U_M^x and we define $\cup_{x' \in I} U_M^{x'} = U_M^I$. For a cluster C_i , for each image $x \in I$, we obtain the average of personalized saliency maps for image x (taken from PSM dataset) for all individuals in C_i , and call this image $AvgSal_{C_i}^x$. The target dataset for I2I model for cluster C_i will be $\cup_{x' \in I} AvgSal_{C_i}^{x'} = AvgSal_{C_i}^I$. So for each cluster C_i , the source domain is $A = U_M^I$ and the target domain is $B_i = AvgSal_{C_i}^I$. In the Pix2Pix model, which is a supervised model, the pairs of source and target images are U_M^x and $AvgSal_{C_i}^x$, for all $x \in I$.

Then, for each cluster C_i we train an I2I model $G_{A \rightarrow B_i}^i$. For an input image $x_A \in A$, the model generates x_{A, B_i} , which is indistinguishable from image $x_{B_i} \in B_i$. The mathematical formulation of our problem is as below:

$$\forall i \in \{1, 2, \dots, n\}, x_{A, B_i} \in B_i : x_{A, B_i} = G_{A \rightarrow B_i}^i(x_A) \quad (2)$$

G. Prediction of saliency map for a new individual

In this part we describe how to predict clustered saliency maps for a new individual, having a dataset D of personalized saliency data. First, using the Subject Similarity Clustering algorithm, we put all the individuals in the dataset D into clusters and we obtain trained I2I models for each cluster, as we explained in Section III-E.

Now we want to determine, for a new individual A , which cluster this person belongs to, given their personal features and any available saliency maps for A . Assume that from A , we have the vector for a set of features, F , and a set S of A 's saliency maps for the set of images, I , such that all $x \in I$ exist

| Setting | | Gender | Fashion | Colors | Sports | Other |
|-----------------|----------------------------------|--------|---------|--------|--------|-------|
| All individuals | Average of pairwise similarities | 48.5% | 65.2% | 73.3% | 64.7% | 72.3% |
| | Median of pairwise similarities | 0.0% | 63.6% | 75.0% | 63.6% | 75.0% |
| Setting 0 | Cluster 1 | 47.0% | 64.0% | 72.6% | 65.2% | 62.9% |
| | Cluster 2 | 56.4% | 61.3% | 76.6% | 69.9% | 71.8% |
| | Cluster 3 | 71.4% | 74.0% | 68.5% | 71.4% | 92.9% |
| | Average | 58.3% | 66.4% | 72.6% | 68.8% | 75.9% |
| Setting 1 | Cluster 1 | 47.0% | 65.8% | 72.8% | 66.9% | 65.9% |
| | Cluster 2 | 53.3% | 59.2% | 75.8% | 68.5% | 74.4% |
| | Cluster 3 | 57.1% | 72.7% | 72.8% | 62.3% | 76.8% |
| | Average | 52.5% | 65.9% | 73.8% | 65.9% | 72.4% |
| Setting 2 | Cluster 1 | 46.2% | 64.8% | 72.6% | 64.3% | 64.7% |
| | Cluster 2 | 46.7% | 64.0% | 75.7% | 69.5% | 78.3% |
| | Cluster 3 | 42.9% | 61.9% | 71.4% | 61.0% | 78.6% |
| | Average | 45.3% | 63.6% | 73.2% | 64.9% | 73.9% |
| Setting 3 | Cluster 1 | 47.0% | 64.0% | 72.6% | 65.2% | 62.9% |
| | Cluster 2 | 51.5% | 63.2% | 76.6% | 69.3% | 73.9% |
| | Cluster 3 | 66.7% | 72.1% | 67.9% | 68.5% | 91.7% |
| | Average | 55.1% | 66.4% | 72.4% | 67.7% | 76.2% |
| Setting 4 | Cluster 1 | 47.0% | 64.0% | 72.6% | 65.2% | 62.9% |
| | Cluster 2 | 56.4% | 61.3% | 76.6% | 69.9% | 71.8% |
| | Cluster 3 | 71.4% | 74.0% | 68.5% | 71.4% | 92.9% |
| | Average | 58.3% | 66.4% | 72.6% | 68.8% | 75.9% |
| Setting 5 | Cluster 1 | 58.1% | 60.3% | 72.3% | 70.6% | 73.3% |
| | Cluster 2 | 42.9% | 74.0% | 78.0% | 70.6% | 73.8% |
| | Cluster 3 | 57.1% | 79.5% | 77.0% | 64.0% | 76.8% |
| | Average | 52.7% | 71.3% | 75.8% | 68.4% | 74.6% |
| Setting 6 | Cluster 1 | 52.4% | 77.5% | 81.0% | 67.1% | 92.9% |
| | Cluster 2 | 100.0% | 71.4% | 77.4% | 79.2% | 78.6% |
| | Cluster 3 | 46.4% | 62.3% | 71.7% | 62.0% | 62.5% |
| | Cluster 4 | 57.1% | 72.1% | 77.2% | 64.9% | 76.8% |
| | Average | 64.0% | 70.8% | 76.8% | 68.3% | 77.7% |

TABLE III: Percentage of similarity of features in different categories for all pairs of individuals in each cluster in each clustering setting. For setting "All individuals" we have included the "Average of pairwise similarities" and "Median of pairwise similarities" for all pairs of individuals in PSM dataset. "Average" in the last row of each setting is the average of the similarities for each feature category for all the clusters in that setting.

in D . First we define a closeness measure between individual A and each cluster C_i , called $Closeness(A, C_i)$. We compute this similarity in the following way. At the beginning, for all the clusters C_i , $Closeness(A, C_i) = 0$. For each image $x \in I$, we find the L_1 distance between personalized saliency map of A for image x , and $AvgSal_{C_i}^x$ for each cluster C_i , and for the cluster C_{min} with the least distance, we increase $Closeness(A, C_{min})$ by 1. After this, we add the effect of features to the closeness measure. For each individual in dataset D , as the feature vector we only consider the subvector of the features in F . For each cluster C_i , we get the mean of the feature subvectors for all individuals in C_i . Then we find the cluster C_{fmin} which its mean feature subvector has the least L_1 distance from feature vector of A . Then we increase $Closeness(A, C_{fmin})$ by the feature weights W that we specified in Section III-C. Finally, we assign A to the cluster C such that $Closeness(A, C)$ is the maximum among

all the clusters.

To predict the saliency map of A for an image x , we obtain the universal saliency map for x , using a universal saliency prediction model. Given the trained I2I model for A 's cluster, for the image x , we can translate x 's universal saliency map to saliency map for A 's cluster, which we consider as the predicted saliency map for A . You can see the pipeline of the process of clustering and I2I translation in Fig. 3.

IV. EXPERIMENTAL RESULTS

In this section, we describe experiments to test the performance of our proposed methods in comparison to some state-of-the-art universal saliency detection methods. For choosing a suitable I2I model, we test and compare two approaches, UNIT model and Pix2Pix model.

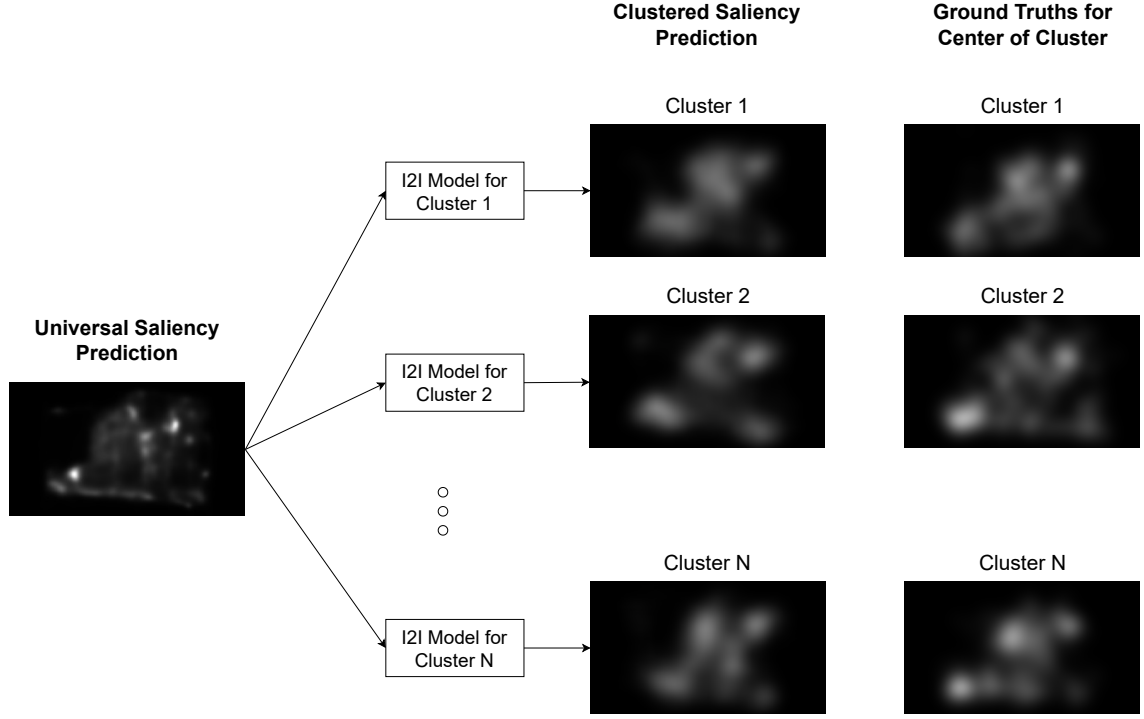


Fig. 2: General overview of the process of converting universal saliency maps to clustered saliency maps using an I2I model for each cluster. Ground truths for the center of a cluster are averages of ground truth saliency maps of all individuals in that cluster.

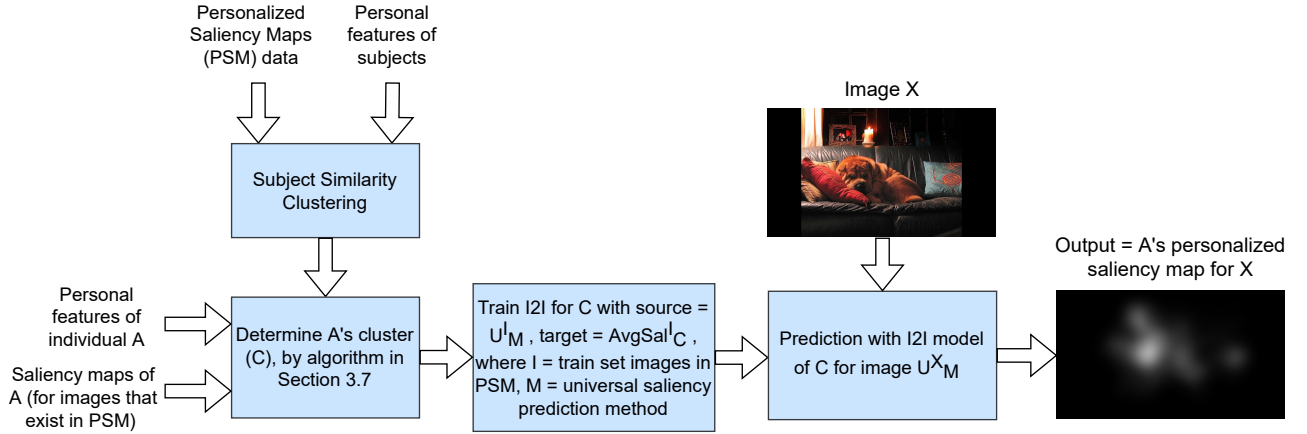


Fig. 3: The pipeline of our clustered saliency prediction model, which is combined from clustering and image-to-image translation.

A. UNIT approach

We tested the UNIT model using the same hyperparameters, batch size and number of iterations as the original paper [63]. We performed clustering using the Subject Similarity Clustering algorithm, with features weight equal to 0 and $K = 5$. For all the clusters of individuals, we constructed source and target sets as explained in Section III-F and trained the UNIT model on each cluster and evaluated the results. In another experiment, we used the Pix2Pix model for image-to-image translation in order to compare the performance

of UNIT and Pix2Pix as I2I model in the same setting of clustering. In both cases using UNIT and Pix2Pix, we used DeepGaze II to obtain the universal saliency maps that are used as the source images for I2I. In Table IV, you can see the performance of DeepGaze II and performances of clustered saliency prediction using I2I models UNIT and Pix2Pix. In this part of experiments, the test set split size is 15% of all the images. The evaluation results in Table IV for each method (universal, UNIT and Pix2Pix), for each cluster C , are the average of scores for all person P in C , where ground

| Method | | CC | SIM | AUC Judd | NSS |
|-----------|-----------|------|------|----------|------|
| Universal | Cluster 1 | 0.50 | 0.50 | 0.86 | 2.32 |
| | Cluster 2 | 0.53 | 0.51 | 0.88 | 2.29 |
| | Cluster 3 | 0.50 | 0.48 | 0.89 | 2.47 |
| | Average | 0.51 | 0.50 | 0.88 | 2.36 |
| UNIT | Cluster 1 | 0.67 | 0.61 | 0.86 | 1.95 |
| | Cluster 2 | 0.72 | 0.63 | 0.89 | 2.18 |
| | Cluster 3 | 0.69 | 0.59 | 0.90 | 2.31 |
| | Average | 0.69 | 0.61 | 0.88 | 2.15 |
| Pix2Pix | Cluster 1 | 0.66 | 0.60 | 0.86 | 1.97 |
| | Cluster 2 | 0.71 | 0.63 | 0.88 | 2.18 |
| | Cluster 3 | 0.67 | 0.59 | 0.89 | 2.27 |
| | Average | 0.68 | 0.61 | 0.88 | 2.14 |

TABLE IV: Comparison of performance of DeepGaze II universal saliency, DeepGaze II based clustered saliency using UNIT as I2I model and DeepGaze II based clustered saliency using Pix2Pix as I2I model. "Average" in the last row of each method, is the average of the scores for all the clusters. Higher score indicates a better performance in all metrics.

truths are personalized saliency maps of P and inputs of saliency metrics functions are the prediction results by the corresponding method. The "Average" row in each method, contains the average scores across all clusters in that method.

As you can see, the performance in all metrics except NSS for predictions of saliency maps using either of UNIT or Pix2Pix as I2I model is higher than the performance of DeepGaze II universal saliency method.

For this setting of clustering, training the UNIT model using an NVIDIA Titan Xp GPU for all the clusters took more than a week. Training the Pix2Pix model for all clusters using the same machine, takes less than a day. Since the performance metrics using UNIT and Pix2Pix are very close to each other as you can see in Table IV, and considering the substantial difference between training time of these two methods, we will use Pix2Pix model to perform the rest of our experiments on other settings of clustering. Also since we have all the image pairs for training I2I in our dataset, the supervised nature of Pix2Pix does not impose any limitations on us.

B. Pix2Pix

As mentioned in Section IV-A, for the rest of our experiments we have chosen Pix2Pix as our main method for obtaining clustered saliency maps from universal saliency maps. Here we used Pix2Pix with source and target sets described in Section III-F. Pix2Pix was trained for 100 epochs and a batch size of 1. The rest of the hyperparameters and settings of Pix2Pix are same as the original paper [64]. For performing the experiments in this section, we used clustering settings 0 to 6, where their properties can be seen in Table II. Note that in order to be able to compare different clustering settings here, we have used the same 100 initial images for Subject Similarity Clustering in all of these settings. Also, all

the settings use the same train set and same test set. The split size for test set images is 20%.

We ran 3 different set of experiments, where in each set we use one of DeepGaze II, ML-Net and SalGAN, to obtain universal saliency maps, as the source images for Pix2Pix model. In Fig. 4, you see the universal saliency maps of a random stimuli, and the clustered predictions using each of universal saliency models, for Setting 4. You can see the evaluation results of using DeepGaze II based clustered saliency prediction, ML-Net based clustered saliency prediction and SalGAN based clustered saliency prediction, in Tables V and VI, Tables VII and VIII, Tables IX and X, respectively.

The evaluation results in these tables for each clustering setting, for each cluster C , for the "Clustered" method, are the average of scores for all person P in C , where ground truths are personalized saliency maps of P and inputs of saliency metrics functions are the prediction results by our clustered saliency prediction method for cluster C . Also for the "Universal", for each cluster C , the scores are the average of scores for all person P in C , where ground truths are personalized saliency maps of P and inputs of saliency metrics functions are the predictions by the corresponding universal saliency method in that table. The "Average" row in each clustering settings, contains the average scores across all clusters in that setting, for each of Clustered and Universal methods.

As you can see in Tables V, VI, VII, VIII, IX and X, across all the setting, the results for CC, SIM and AUC Judd metrics for nearly all the cases are higher in the clustered saliency predictions, than the results of universal saliency predictions. This shows the improvement of our model over universal saliency prediction models.

In each experiment case of DeepGaze II, ML-Net and SalGAN as the base universal saliency model, we have evaluated the results on two baseline models. In the first baseline model, our clustering of individuals is random, where we assign each person randomly to one of 3 clusters, based on uniform distribution. In the second baseline model we have only one cluster, which is comprised of all the individuals.

As you can see in Tables V, VI, VII and VIII, for DeepGaze II based clustered saliency prediction and for ML-Net based clustered saliency prediction, in all the clustering settings except Settings 5 and 6, the average performance is higher than the performance for two baseline models. Based on Tables IX and X, for SalGAN based clustered saliency prediction, in all the clustering settings except Settings 4 and 5 and 6, the average performance is higher than the performance for two baseline models.

This shows that higher features weights negatively affect the performance of clustered saliency prediction. Thus, the Subject Similarity Clustering algorithm using the proper feature weights, effectively contributes to the saliency prediction accuracy.

We see that for some cases, the performance in NSS for the universal saliency model is higher than the performance for the clustered predictions using trained I2I model. The reason

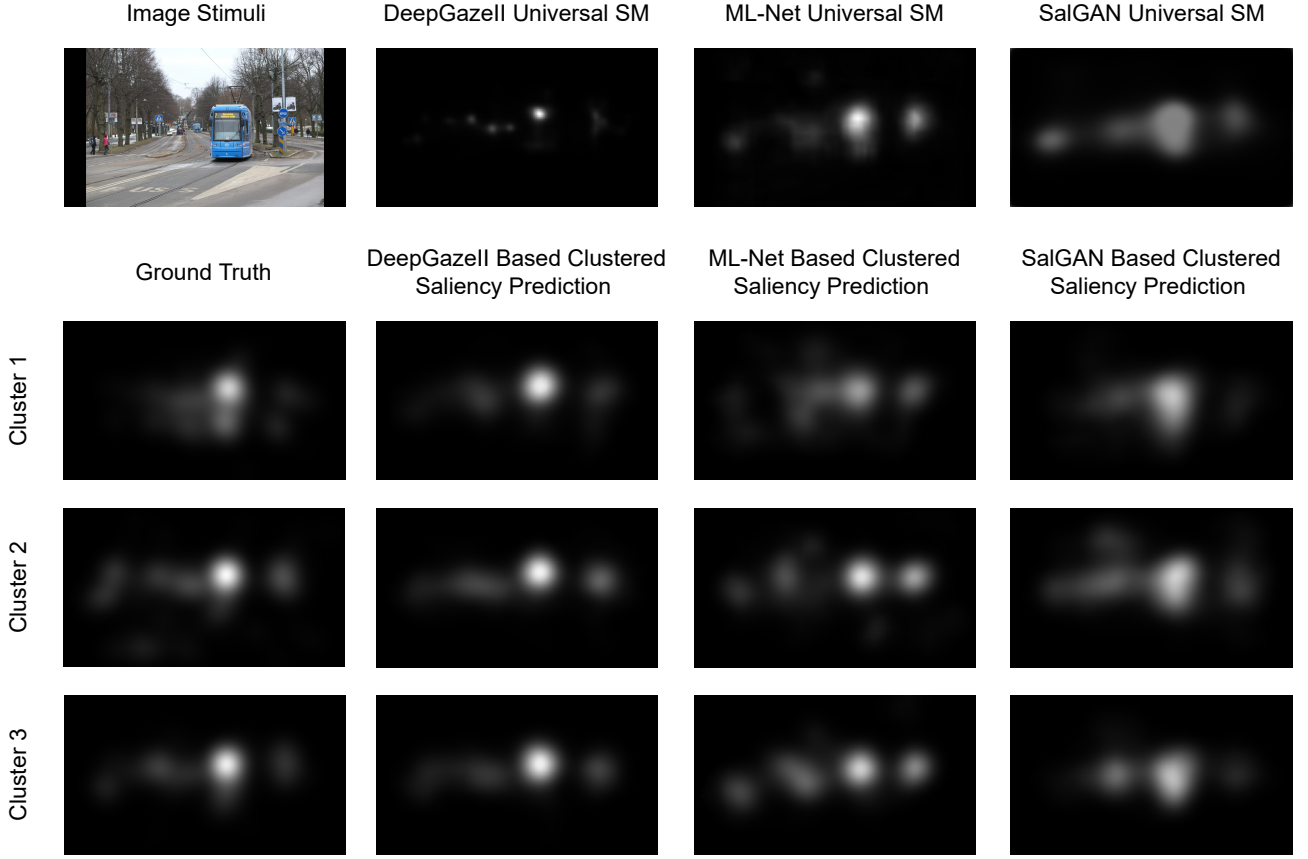


Fig. 4: Clustered saliency prediction for the depicted stimuli image for clusters in Setting 4, using different universal saliency prediction methods as the base for I2I model. Here "SM" stands for Saliency Map.

is that the I2I models are trained to convert universal saliency maps to saliency maps of a cluster and they don't take into account the fixation maps, while in evaluating the results with NSS, we compare the predicted saliency maps against the fixation maps. So considering this, NSS would not be a good metric for our evaluations. As we can see in Fig. 4, in the universal saliency maps for DeepGaze II, the salient parts are more sharp than the salient parts in the predictions for each cluster. Since NSS penalizes false positives at fixation locations, a more sharp saliency map which has higher peaks, might gain a higher NSS than a saliency map with more spread-out salient regions.

In order to study more deeply the effect of different personal features on the clustering and performance of clustered saliency prediction, we ran experiments where in each experiment we consider one of five different personal features categories for our Subject Similarity Clustering algorithm. Also, in additional experiments we consider every combination of two different categories of personal features for Subject Similarity Clustering algorithm. In all of these experiments, we use the ML-Net approach for universal saliency prediction, since based on Tables V, VI, VII, VIII, IX and X, the saliency scores of our model using ML-Net for producing source images for I2I are higher than the scores using the other two

saliency methods. Also, we set the features weights as 0.5, since in Table VII Setting 2 with features weight equal to 0.5 has higher scores, compared to all other settings. Also in all of these settings, same 100 initial images for Subject Similarity Clustering, same train sets and same test sets as the experiments in Tables V, VI, VII, VIII, IX and X, were used. The results of these experiments can be seen in Tables XI, XII, XIII.

As can be seen in Tables XI, XII and XIII, we see that SETT(Color) and settings SETT(Fashion) and also SETT(Other) have the highest scores in average.

C. Prediction of saliency for a new person

In order to test our proposed approach in part III-G, for each of the 30 individuals in the PSM dataset, we hold this individual out and consider it as a new person. Then we cluster the 29 other individuals using the Subject Similarity Clustering algorithm. For clustering, we use the same parameters as Setting 2 in Table II for Subject Similarity Clustering algorithm, where features weight is 0.5 and we use all the features. For all 30 different experiments, we use ML-Net as the universal saliency prediction method, as the source set for Pix2Pix-GAN model for each cluster.

| Setting | | Prediction method | CC | SIM | AUC Judd | NSS |
|-----------------|-----------|-------------------|---------------|---------------|---------------|---------------|
| All individuals | Cluster 1 | Clustered | 0.6582 | 0.5924 | 0.8712 | 2.0398 |
| | | Universal | 0.4999 | 0.4905 | 0.8721 | 2.3019 |
| Random assign | Cluster 1 | Clustered | 0.6679 | 0.5969 | 0.8767 | 2.1114 |
| | | Universal | 0.5118 | 0.4975 | 0.8840 | 2.4071 |
| | Cluster 2 | Clustered | 0.6497 | 0.5854 | 0.8715 | 2.0127 |
| | | Universal | 0.4955 | 0.4878 | 0.8742 | 2.3138 |
| | Cluster 3 | Clustered | 0.6541 | 0.5895 | 0.8584 | 1.9650 |
| | | Universal | 0.4956 | 0.4882 | 0.8599 | 2.2035 |
| Setting 0 | Cluster 1 | Clustered | 0.6572 | 0.5906 | 0.8689 | 2.0297 |
| | | Universal | 0.5010 | 0.4912 | 0.8727 | 2.3081 |
| | Cluster 2 | Clustered | 0.6777 | 0.6027 | 0.8857 | 2.2160 |
| | | Universal | 0.5096 | 0.4977 | 0.8855 | 2.3587 |
| | Cluster 3 | Clustered | 0.6609 | 0.6044 | 0.8570 | 1.8968 |
| | | Universal | 0.4982 | 0.4925 | 0.8601 | 2.3028 |
| Setting 1 | Cluster 1 | Clustered | 0.6500 | 0.5788 | 0.8780 | 2.0905 |
| | | Universal | 0.4875 | 0.4757 | 0.8714 | 2.2112 |
| | Cluster 2 | Clustered | 0.6629 | 0.5953 | 0.8736 | 2.0678 |
| | | Universal | 0.4984 | 0.4886 | 0.8723 | 2.2909 |
| | Average | Clustered | 0.6777 | 0.6027 | 0.8857 | 2.2160 |
| | | Universal | 0.5096 | 0.4977 | 0.8855 | 2.3587 |
| Setting 2 | Cluster 1 | Clustered | 0.6780 | 0.6054 | 0.8570 | 1.8968 |
| | | Universal | 0.5109 | 0.5008 | 0.8836 | 2.3026 |
| | Cluster 2 | Clustered | 0.6508 | 0.5791 | 0.8793 | 2.1075 |
| | | Universal | 0.4897 | 0.4768 | 0.8747 | 2.2591 |
| | Average | Clustered | 0.6619 | 0.5950 | 0.8724 | 2.0527 |
| | | Universal | 0.4994 | 0.4896 | 0.8730 | 2.2972 |
| Setting 3 | Cluster 1 | Clustered | 0.6570 | 0.6006 | 0.8541 | 1.9054 |
| | | Universal | 0.4975 | 0.4911 | 0.8607 | 2.3298 |
| | Cluster 2 | Clustered | 0.6780 | 0.6054 | 0.8837 | 2.1451 |
| | | Universal | 0.5109 | 0.5008 | 0.8836 | 2.3026 |
| | Cluster 3 | Clustered | 0.6508 | 0.5791 | 0.8793 | 2.1075 |
| | | Universal | 0.4897 | 0.4768 | 0.8747 | 2.2591 |
| Setting 4 | Cluster 1 | Clustered | 0.6619 | 0.5950 | 0.8724 | 2.0527 |
| | | Universal | 0.4994 | 0.4896 | 0.8730 | 2.2972 |
| | Cluster 2 | Clustered | 0.6675 | 0.5859 | 0.8897 | 2.3000 |
| | | Universal | 0.4981 | 0.4780 | 0.8845 | 2.3716 |
| | Cluster 3 | Clustered | 0.6632 | 0.6036 | 0.8560 | 1.9292 |
| | | Universal | 0.5013 | 0.4936 | 0.8620 | 2.3397 |
| Setting 5 | Cluster 1 | Clustered | 0.6615 | 0.5969 | 0.8776 | 2.0261 |
| | | Universal | 0.4993 | 0.4953 | 0.8764 | 2.2040 |
| | Cluster 2 | Clustered | 0.6641 | 0.5955 | 0.8744 | 2.0851 |
| | | Universal | 0.4996 | 0.4890 | 0.8743 | 2.3051 |
| | Average | Clustered | 0.6605 | 0.5857 | 0.8851 | 2.1904 |
| | | Universal | 0.5026 | 0.4814 | 0.8811 | 2.3319 |
| Setting 6 | Cluster 1 | Clustered | 0.6577 | 0.6014 | 0.8547 | 1.9303 |
| | | Universal | 0.4982 | 0.4925 | 0.8601 | 2.3028 |
| | Cluster 2 | Clustered | 0.6688 | 0.5970 | 0.8814 | 2.1175 |
| | | Universal | 0.5003 | 0.4930 | 0.8795 | 2.2860 |
| | Average | Clustered | 0.6623 | 0.5947 | 0.8737 | 2.0794 |
| | | Universal | 0.5004 | 0.4890 | 0.8736 | 2.3069 |

TABLE V: Comparison of performance of DeepGaze II Universal saliency and DeepGaze II based clustered saliency prediction, using Pix2Pix as I2I model. "Average" in the last row of each setting is the average of the scores for all the clusters in that setting. Setting "All individuals" is the setting where all individuals are in the same cluster and Setting "Random assign" is the setting where each individual is assigned randomly to one of three clusters. Higher score indicates a better performance in all metrics.

In each of 30 experiments, we assign the new person to its appropriate cluster, based on the algorithm described in Section III-G, under two different scenarios. In the first scenario, as available information for the new person, we use all the personal features and all the person's saliency maps of

images in test set that we used for training the I2I models in our algorithm. In the second scenario, we assume we only have personal features of the new person and we have no previous saliency maps of this person.

For each of the scenarios, we evaluated the results obtained

| Setting | | Prediction method | CC | SIM | AUC Judd | NSS |
|------------|-----------|-------------------|---------------|---------------|---------------|---------------|
| Setting 4 | Cluster 1 | Clustered | 0.6767 | 0.6008 | 0.8839 | 2.1877 |
| | | Universal | 0.5096 | 0.4977 | 0.8855 | 2.3587 |
| | Cluster 2 | Clustered | 0.6503 | 0.5798 | 0.8783 | 2.0567 |
| | | Universal | 0.4875 | 0.4757 | 0.8714 | 2.2112 |
| Setting 5 | Cluster 3 | Clustered | 0.6573 | 0.6016 | 0.8554 | 1.9008 |
| | | Universal | 0.4982 | 0.4925 | 0.8601 | 2.3028 |
| | Average | Clustered | 0.6614 | 0.5941 | 0.8725 | 2.0484 |
| | | Universal | 0.4984 | 0.4886 | 0.8723 | 2.2909 |
| Setting 6 | Cluster 1 | Clustered | 0.6612 | 0.5949 | 0.8717 | 2.0645 |
| | | Universal | 0.5057 | 0.4956 | 0.8761 | 2.3777 |
| | Cluster 2 | Clustered | 0.6728 | 0.6066 | 0.8711 | 1.9917 |
| | | Universal | 0.5105 | 0.5007 | 0.8774 | 2.3278 |
| Setting 7 | Cluster 3 | Clustered | 0.6508 | 0.5760 | 0.8682 | 2.0245 |
| | | Universal | 0.4798 | 0.4720 | 0.8599 | 2.1370 |
| | Average | Clustered | 0.6616 | 0.5925 | 0.8703 | 2.0269 |
| | | Universal | 0.4987 | 0.4894 | 0.8711 | 2.2808 |
| Setting 8 | Cluster 1 | Clustered | 0.6590 | 0.5906 | 0.8714 | 2.0184 |
| | | Universal | 0.5009 | 0.4919 | 0.8712 | 2.2512 |
| | Cluster 2 | Clustered | 0.6634 | 0.5926 | 0.8769 | 2.1252 |
| | | Universal | 0.5130 | 0.4953 | 0.8831 | 2.5275 |
| Setting 9 | Cluster 3 | Clustered | 0.6241 | 0.5705 | 0.8542 | 1.9127 |
| | | Universal | 0.4816 | 0.4788 | 0.8573 | 2.2269 |
| | Cluster 4 | Clustered | 0.6662 | 0.5990 | 0.8756 | 2.0170 |
| | | Universal | 0.5058 | 0.4967 | 0.8780 | 2.2239 |
| Setting 10 | Average | Clustered | 0.6532 | 0.5882 | 0.8695 | 2.0183 |
| | | Universal | 0.5003 | 0.4907 | 0.8724 | 2.3074 |

TABLE VI: Continuation of Table V.

by assigning the new person to the cluster chosen by our algorithm. We compared these scores to the evaluation scores obtained by assigning the new person to the non-chosen clusters. For each of the 30 experiments, we averaged the scores of assigning the new person to the chosen cluster and also we averaged all the scores of assigning the new person to each of the non-chosen clusters. The results for first scenario and second scenario can be seen in Table XIV and Table XV, respectively.

As we see in the first scenario, the average of scores over all experiments for assigning the new person to chosen cluster in CC is higher than the average of scores for all non-chosen clusters. In the second scenario, the average of scores for CC and SIM for chosen clusters is higher than the non-chosen clusters. In both scenarios, the average scores for AUC Judd and NSS is higher in universal prediction for chosen cluster. As explained in Section IV-B, for NSS and sometimes for AUC Judd the scores are not stable and higher in the universal prediction, because these two metrics consider fixation points, while in training the I2I model we consider saliency maps. It is worth noting that the scores for these two metrics are still higher in the chosen cluster.

Based on these observations, we see that using only features in this case led to better estimation of the appropriate cluster for each new observer.

V. DISCUSSION

As we see in Table III, in Setting 6 we have the highest average of personal features similarities across all the clusters. As can be seen in Table II, for Subject Similarity Clustering, this setting has the highest personal features weight, among all the settings. This explains the higher similarities of personal features through clusters for this setting and shows that our clustering approach does a good job in putting individuals with similar features in the same cluster.

It can be seen that for DeepGaze II based and ML-Net based clustered saliency predictions in Tables V, VI, VII and VIII, Setting 2 has the highest scores and for SalGAN based clustered saliency predictions in Table IX, Setting 1 and Setting 2 has the best performance among all the settings. Based on Table II, for Setting 2, the weight of personal features is 0.5 for Subject Similarity Clustering. We can see that in other settings with higher or lower feature weights, the saliency scores decrease. This shows that increasing feature weights after a certain threshold will cause in the decline of quality of the clusters. Also, decreasing the feature weights below an optimal point, diminishes the optimal effect that features have in this case.

Based on the results in Tables XI, XII and XIII, we can conclude that feature categories Color, Fashion and Other are the most correlated with the saliency prediction of people

| Setting | | Prediction method | CC | SIM | AUC Judd | NSS |
|-----------------|-----------|-------------------|---------------|---------------|---------------|---------------|
| All individuals | Cluster 1 | Clustered | 0.6832 | 0.6076 | 0.8746 | 2.1003 |
| | | Universal | 0.6405 | 0.5690 | 0.8706 | 2.1942 |
| Random assign | Cluster 1 | Clustered | 0.6944 | 0.6131 | 0.8813 | 2.1806 |
| | | Universal | 0.6543 | 0.5737 | 0.8810 | 2.2971 |
| | Cluster 2 | Clustered | 0.6712 | 0.5994 | 0.8730 | 2.0896 |
| | | Universal | 0.6317 | 0.5630 | 0.8717 | 2.1914 |
| | Average | Clustered | 0.6808 | 0.6049 | 0.8726 | 2.0855 |
| | | Universal | 0.6420 | 0.5697 | 0.8712 | 2.2013 |
| Setting 0 | Cluster 1 | Clustered | 0.7121 | 0.6246 | 0.8884 | 2.2917 |
| | | Universal | 0.6493 | 0.5679 | 0.8827 | 2.3414 |
| | Cluster 2 | Clustered | 0.6802 | 0.6135 | 0.8584 | 1.9871 |
| | | Universal | 0.6600 | 0.5928 | 0.8619 | 2.1101 |
| | Average | Clustered | 0.6744 | 0.5939 | 0.8769 | 2.1494 |
| | | Universal | 0.5930 | 0.5299 | 0.8666 | 2.1071 |
| Setting 1 | Cluster 1 | Clustered | 0.6815 | 0.6142 | 0.8606 | 1.9898 |
| | | Universal | 0.6584 | 0.5913 | 0.8619 | 2.1144 |
| | Cluster 2 | Clustered | 0.7109 | 0.6265 | 0.8872 | 2.2517 |
| | | Universal | 0.6472 | 0.5703 | 0.8802 | 2.2780 |
| | Average | Clustered | 0.6876 | 0.6004 | 0.8834 | 2.2267 |
| | | Universal | 0.6050 | 0.5337 | 0.8716 | 2.2094 |
| Setting 2 | Cluster 1 | Clustered | 0.6952 | 0.6053 | 0.8914 | 2.3269 |
| | | Universal | 0.6207 | 0.5366 | 0.8808 | 2.3239 |
| | Cluster 2 | Clustered | 0.6809 | 0.6144 | 0.8594 | 1.9702 |
| | | Universal | 0.6593 | 0.5915 | 0.8629 | 2.1282 |
| | Average | Clustered | 0.7020 | 0.6220 | 0.8821 | 2.1713 |
| | | Universal | 0.6297 | 0.5623 | 0.8736 | 2.1893 |
| Setting 3 | Cluster 1 | Clustered | 0.6901 | 0.6030 | 0.8859 | 2.2527 |
| | | Universal | 0.6087 | 0.5347 | 0.8750 | 2.2009 |
| | Cluster 2 | Clustered | 0.6845 | 0.6173 | 0.8579 | 1.9529 |
| | | Universal | 0.6600 | 0.5928 | 0.8619 | 2.1101 |
| | Average | Clustered | 0.7014 | 0.6176 | 0.8857 | 2.2259 |
| | | Universal | 0.6368 | 0.5624 | 0.8772 | 2.2750 |
| | Average | Clustered | 0.6920 | 0.6126 | 0.8765 | 2.1438 |
| | | Universal | 0.6352 | 0.5633 | 0.8714 | 2.1953 |

TABLE VII: Comparison of performance of ML-Net Universal saliency and ML-Net based clustered saliency prediction, using Pix2Pix as I2I model. "Average" in the last row of each setting is the average of the scores for all the clusters in that setting. Setting "All individuals" is the setting where all individuals are in the same cluster and Setting "Random assign" is the setting where each individual is assigned randomly to one of three clusters. Higher score indicates a better performance in all metrics.

in this dataset. This is reasonable, since colors in an image are known to have a significant effect in drawing attention. Also, individuals preference in fashion might manifest in their attention patterns.

One of the advantages of our clustered saliency prediction model is that the universal saliency maps that we use as the

base, can be obtained with any universal saliency model. So as universal saliency models improve, we can upgrade our model by using a better performing universal saliency model base.

| Setting | | Prediction method | CC | SIM | AUC Judd | NSS |
|-----------|-----------|-------------------|---------------|---------------|---------------|---------------|
| Setting 4 | Cluster 1 | Clustered | 0.7088 | 0.6215 | 0.8888 | 2.2902 |
| | | Universal | 0.6493 | 0.5679 | 0.8827 | 2.3414 |
| | Cluster 2 | Clustered | 0.6680 | 0.5885 | 0.8767 | 2.1345 |
| | | Universal | 0.5930 | 0.5299 | 0.8666 | 2.1071 |
| | Cluster 3 | Clustered | 0.6835 | 0.6167 | 0.8602 | 2.0003 |
| | | Universal | 0.6600 | 0.5928 | 0.8619 | 2.1101 |
| | Average | Clustered | 0.6868 | 0.6089 | 0.8752 | 2.1417 |
| | | Universal | 0.6341 | 0.5635 | 0.8704 | 2.1862 |
| Setting 5 | Cluster 1 | Clustered | 0.6928 | 0.6155 | 0.8770 | 2.1168 |
| | | Universal | 0.6511 | 0.5778 | 0.8739 | 2.2351 |
| | Cluster 2 | Clustered | 0.6861 | 0.6141 | 0.8712 | 2.0487 |
| | | Universal | 0.6531 | 0.5813 | 0.8741 | 2.1776 |
| | Cluster 3 | Clustered | 0.6798 | 0.5947 | 0.8722 | 2.1286 |
| | | Universal | 0.6095 | 0.5417 | 0.8615 | 2.1322 |
| | Average | Clustered | 0.6862 | 0.6081 | 0.8735 | 2.0980 |
| | | Universal | 0.6379 | 0.5669 | 0.8698 | 2.1816 |
| Setting 6 | Cluster 1 | Clustered | 0.6878 | 0.6078 | 0.8747 | 2.0905 |
| | | Universal | 0.6322 | 0.5645 | 0.8663 | 2.1605 |
| | Cluster 2 | Clustered | 0.6958 | 0.6119 | 0.8811 | 2.2180 |
| | | Universal | 0.6636 | 0.5780 | 0.8831 | 2.3691 |
| | Cluster 3 | Clustered | 0.6673 | 0.5955 | 0.8608 | 2.0153 |
| | | Universal | 0.6354 | 0.5690 | 0.8609 | 2.1363 |
| | Cluster 4 | Clustered | 0.6830 | 0.6096 | 0.8765 | 2.0582 |
| | | Universal | 0.6325 | 0.5650 | 0.8733 | 2.1286 |
| | Average | Clustered | 0.6835 | 0.6062 | 0.8733 | 2.0955 |
| | | Universal | 0.6409 | 0.5691 | 0.8709 | 2.1986 |

TABLE VIII: Continuation of Table VII.

VI. CONCLUSION AND FUTURE WORK

From our experiments, we conclude that our clustered saliency prediction method improves upon standard universal saliency prediction methods. Also, as we discussed in Section IV-B, our Subject Similarity Clustering approach given the proper feature weights, divides the individuals into clusters, where each cluster contains individuals with more similar saliency patterns. We also see that some features categories such as color and fashion, appear to correlate more with the saliency of individuals.

Even though the findings in this paper unravel the effects of different factors in saliency prediction for groups of people in the PSM dataset, the limited features and diversity in the demographics of individuals in this dataset has a negative effect on finding more explanatory clusters. Also, the features used in this dataset are not distinctive enough between different individuals, and the feature vectors of different individuals can have a lot of common parts. As a result, we can say that these features are not descriptive enough of the attention patterns of individuals. These factors contribute to the noisiness of clusters. With an improved dataset with more descriptive personal features, our methods might even appear more effective.

For future work, building a personal saliency maps dataset with an improved set of personal features and more diversity in the demographics of the subjects can be very helpful for

unraveling different effects in saliency prediction. Considering there are very few datasets in the area of personalized saliency prediction, a new dataset with the mentioned improved aspects can help the progress in this area by a lot.

Since the attention of individuals can be affected immensely if they are searching for a target object in the image (i.e. visual search), it will also be useful to explore clustered saliency prediction in visual search tasks.

ACKNOWLEDGMENTS

This research was supported by a CFREF-IVADO grant. All authors have read and agreed to the published version of the manuscript.

REFERENCES

- [1] T. Judd, K. Ehinger, F. Durand, and A. Torralba, "Learning to predict where humans look," in *2009 IEEE 12th International Conference on Computer Vision*, 2009, pp. 2106–2113.
- [2] M. Jiang, S. Huang, J. Duan, and Q. Zhao, "Salicon: Saliency in context," in *Proceedings of the IEEE conference on computer vision and pattern recognition*, 2015, pp. 1072–1080.
- [3] N. W. Kim, Z. Bylinskii, M. A. Borkin, K. Z. Gajos, A. Oliva, F. Durand, and H. Pfister, "Bubbleview: an interface for crowdsourcing image importance maps and tracking visual attention," *ACM Transactions on Computer-Human Interaction (TOCHI)*, vol. 24, no. 5, pp. 1–40, 2017.
- [4] K. Krafska, A. Khosla, P. Kellnhofer, H. Kannan, S. Bhandarkar, W. Matusik, and A. Torralba, "Eye tracking for everyone," in *Proceedings of the IEEE conference on computer vision and pattern recognition*, 2016, pp. 2176–2184.

| Setting | | Prediction method | CC | SIM | AUC Judd | NSS |
|-----------------|-----------|-------------------|---------------|---------------|---------------|---------------|
| All individuals | Cluster 1 | Clustered | 0.6695 | 0.5987 | 0.8725 | 2.0187 |
| | | Universal | 0.6520 | 0.5797 | 0.8737 | 1.9816 |
| Random assign | Cluster 1 | Clustered | 0.6796 | 0.6041 | 0.8807 | 2.0623 |
| | | Universal | 0.6656 | 0.5857 | 0.8842 | 2.0631 |
| | Cluster 2 | Clustered | 0.6545 | 0.5871 | 0.8715 | 1.9902 |
| | | Universal | 0.6454 | 0.5743 | 0.8755 | 1.9891 |
| | Cluster 3 | Clustered | 0.6629 | 0.5942 | 0.8616 | 1.9448 |
| | | Universal | 0.6492 | 0.5814 | 0.8632 | 1.9072 |
| | Average | Clustered | 0.6657 | 0.5951 | 0.8713 | 1.9991 |
| | | Universal | 0.6534 | 0.5805 | 0.8743 | 1.9865 |
| Setting 0 | Cluster 1 | Clustered | 0.6937 | 0.6088 | 0.8866 | 2.1914 |
| | | Universal | 0.6567 | 0.5763 | 0.8861 | 2.0733 |
| | Cluster 2 | Clustered | 0.6647 | 0.6051 | 0.8559 | 1.8712 |
| | | Universal | 0.6754 | 0.6071 | 0.8638 | 1.9195 |
| | Cluster 3 | Clustered | 0.6588 | 0.5826 | 0.8749 | 2.0542 |
| | | Universal | 0.6047 | 0.5380 | 0.8712 | 1.9437 |
| | Average | Clustered | 0.6724 | 0.5988 | 0.8725 | 2.0389 |
| | | Universal | 0.6456 | 0.5738 | 0.8737 | 1.9788 |
| Setting 1 | Cluster 1 | Clustered | 0.6629 | 0.6024 | 0.8560 | 1.8929 |
| | | Universal | 0.6726 | 0.6048 | 0.8635 | 1.9194 |
| | Cluster 2 | Clustered | 0.6924 | 0.6117 | 0.8838 | 2.1363 |
| | | Universal | 0.6570 | 0.5808 | 0.8837 | 2.0310 |
| | Cluster 3 | Clustered | 0.6665 | 0.5862 | 0.8803 | 2.1315 |
| | | Universal | 0.6150 | 0.5408 | 0.8766 | 2.0129 |
| | Average | Clustered | 0.6739 | 0.6001 | 0.8734 | 2.0536 |
| | | Universal | 0.6482 | 0.5755 | 0.8746 | 1.9878 |
| Setting 2 | Cluster 1 | Clustered | 0.6703 | 0.5859 | 0.8880 | 2.2385 |
| | | Universal | 0.6244 | 0.5390 | 0.8850 | 2.0946 |
| | Cluster 2 | Clustered | 0.6607 | 0.6016 | 0.8579 | 1.9003 |
| | | Universal | 0.6742 | 0.6056 | 0.8649 | 1.9315 |
| | Cluster 3 | Clustered | 0.6870 | 0.6111 | 0.8808 | 2.0725 |
| | | Universal | 0.6426 | 0.5746 | 0.8772 | 1.9676 |
| | Average | Clustered | 0.6727 | 0.5995 | 0.8756 | 2.0704 |
| | | Universal | 0.6471 | 0.5731 | 0.8757 | 1.9979 |
| Setting 3 | Cluster 1 | Clustered | 0.6646 | 0.5853 | 0.8797 | 2.1484 |
| | | Universal | 0.6181 | 0.5411 | 0.8791 | 2.0190 |
| | Cluster 2 | Clustered | 0.6618 | 0.6044 | 0.8576 | 1.8518 |
| | | Universal | 0.6754 | 0.6071 | 0.8638 | 1.9195 |
| | Cluster 3 | Clustered | 0.6777 | 0.6007 | 0.8814 | 2.1299 |
| | | Universal | 0.6456 | 0.5716 | 0.8809 | 2.0249 |
| | Average | Clustered | 0.6680 | 0.5968 | 0.8729 | 2.0434 |
| | | Universal | 0.6464 | 0.5733 | 0.8746 | 1.9878 |

TABLE IX: Comparison of performance of SalGAN Universal saliency and SalGAN based clustered saliency prediction, using Pix2Pix as I2I model. "Average" in the last row of each setting is the average of the scores for all the setting's clusters. Setting "All individuals" is the setting where all individuals are in the same cluster and Setting "Random assign" is the setting where each individual is assigned randomly to one of three clusters. Higher score indicates a better performance in all metrics.

- [5] L. Itti, C. Koch, and E. Niebur, "A model of saliency-based visual attention for rapid scene analysis," *IEEE Transactions on pattern analysis and machine intelligence*, vol. 20, no. 11, pp. 1254–1259, 1998.
- [6] A. Borji, "Saliency prediction in the deep learning era: Successes and limitations," *IEEE transactions on pattern analysis and machine intelligence*, 2019.
- [7] S. Jain and S. S. Kamath, "Saliency prediction for visual regions of interest with applications in advertising," in *Video Analytics. Face and Facial Expression Recognition and Audience Measurement*. Springer, 2016, pp. 48–60.
- [8] Z. Ma, L. Qing, J. Miao, and X. Chen, "Advertisement evaluation using visual saliency based on foveated image," in *2009 IEEE International Conference on Multimedia and Expo*. IEEE, 2009, pp. 914–917.
- [9] L. A. Leiva, Y. Xue, A. Bansal, H. R. Tavakoli, T. K ro lu, J. Du, N. R. Dayama, and A. Oulasvirta, "Understanding visual saliency in mobile user interfaces," in *22nd International Conference on Human-Computer*

| Setting | | Prediction method | CC | SIM | AUC Judd | NSS |
|-----------|-----------|-------------------|---------------|---------------|---------------|---------------|
| Setting 4 | Cluster 1 | Clustered | 0.6865 | 0.6058 | 0.8840 | 2.1722 |
| | | Universal | 0.6567 | 0.5763 | 0.8861 | 2.0733 |
| | Cluster 2 | Clustered | 0.6481 | 0.5771 | 0.8748 | 2.0291 |
| | | Universal | 0.6047 | 0.5380 | 0.8712 | 1.9437 |
| | Cluster 3 | Clustered | 0.6629 | 0.6049 | 0.8565 | 1.8790 |
| | | Universal | 0.6754 | 0.6071 | 0.8638 | 1.9195 |
| | Average | Clustered | 0.6658 | 0.5959 | 0.8718 | 2.0268 |
| | | Universal | 0.6456 | 0.5738 | 0.8737 | 1.9788 |
| Setting 5 | Cluster 1 | Clustered | 0.6723 | 0.6027 | 0.8739 | 2.0378 |
| | | Universal | 0.6642 | 0.5898 | 0.8770 | 2.0148 |
| | Cluster 2 | Clustered | 0.6687 | 0.6033 | 0.8710 | 1.9319 |
| | | Universal | 0.6667 | 0.5960 | 0.8768 | 1.9705 |
| | Cluster 3 | Clustered | 0.6604 | 0.5800 | 0.8690 | 2.0315 |
| | | Universal | 0.6163 | 0.5464 | 0.8647 | 1.9288 |
| | Average | Clustered | 0.6671 | 0.5953 | 0.8713 | 2.0004 |
| | | Universal | 0.6491 | 0.5774 | 0.8728 | 1.9714 |
| Setting 6 | Cluster 1 | Clustered | 0.6679 | 0.5963 | 0.8717 | 1.9924 |
| | | Universal | 0.6461 | 0.5765 | 0.8712 | 1.9578 |
| | Cluster 2 | Clustered | 0.6759 | 0.5976 | 0.8771 | 2.1333 |
| | | Universal | 0.6691 | 0.5853 | 0.8840 | 2.1005 |
| | Cluster 3 | Clustered | 0.6485 | 0.5842 | 0.8595 | 1.9092 |
| | | Universal | 0.6459 | 0.5772 | 0.8636 | 1.9349 |
| | Cluster 4 | Clustered | 0.6699 | 0.5991 | 0.8739 | 1.9859 |
| | | Universal | 0.6484 | 0.5801 | 0.8770 | 1.9449 |
| | Average | Clustered | 0.6655 | 0.5943 | 0.8706 | 2.0052 |
| | | Universal | 0.6524 | 0.5798 | 0.8740 | 1.9845 |

TABLE X: Continuation of Table IX.

- Interaction with Mobile Devices and Services*, 2020, pp. 1–12.
- [10] M. M. L. Chang, S. K. Ong, and A. Y. C. Nee, “Automatic information positioning scheme in ar-assisted maintenance based on visual saliency,” in *International Conference on Augmented Reality, Virtual Reality and Computer Graphics*. Springer, 2016, pp. 453–462.
- [11] A. M. Treisman and G. Gelade, “A feature-integration theory of attention,” *Cognitive psychology*, vol. 12, no. 1, pp. 97–136, 1980.
- [12] C. Koch and S. Ullman, “Shifts in selective visual attention: towards the underlying neural circuitry,” in *Matters of intelligence*. Springer, 1987, pp. 115–141.
- [13] M. Cerf, E. P. Frady, and C. Koch, “Faces and text attract gaze independent of the task: Experimental data and computer model,” *Journal of vision*, vol. 9, no. 12, pp. 10–10, 2009.
- [14] E. Vig, M. Dorr, and D. Cox, “Large-scale optimization of hierarchical features for saliency prediction in natural images,” in *Proceedings of the IEEE conference on computer vision and pattern recognition*, 2014, pp. 2798–2805.
- [15] M. Kümmerer, L. Theis, and M. Bethge, “Deep gaze i: Boosting saliency prediction with feature maps trained on imagenet,” 2014. [Online]. Available: <https://arxiv.org/abs/1411.1045>
- [16] M. Kümmerer, T. S. A. Wallis, and M. Bethge, “Deepgaze ii: Reading fixations from deep features trained on object recognition,” 2016. [Online]. Available: <https://arxiv.org/abs/1610.01563>
- [17] X. Huang, C. Shen, X. Boix, and Q. Zhao, “Salicon: Reducing the semantic gap in saliency prediction by adapting deep neural networks,” in *Proceedings of the IEEE International Conference on Computer Vision*, 2015, pp. 262–270.
- [18] A. Krizhevsky, I. Sutskever, and G. E. Hinton, “Imagenet classification with deep convolutional neural networks,” *Communications of the ACM*, vol. 60, no. 6, pp. 84–90, 2017.
- [19] K. Simonyan and A. Zisserman, “Very deep convolutional networks for large-scale image recognition,” *arXiv preprint arXiv:1409.1556*, 2014.
- [20] C. Szegedy, W. Liu, Y. Jia, P. Sermanet, S. Reed, D. Anguelov, D. Erhan, V. Vanhoucke, and A. Rabinovich, “Going deeper with convolutions,” in *Proceedings of the IEEE conference on computer vision and pattern recognition*, 2015, pp. 1–9.
- [21] M. Cornia, L. Baraldi, G. Serra, and R. Cucchiara, “A deep multi-level network for saliency prediction,” in *2016 23rd International Conference on Pattern Recognition (ICPR)*. IEEE, 2016, pp. 3488–3493.
- [22] S. S. Kruthiventi, K. Ayush, and R. V. Babu, “Deepfix: A fully convolutional neural network for predicting human eye fixations,” *IEEE Transactions on Image Processing*, vol. 26, no. 9, pp. 4446–4456, 2017.
- [23] J. Pan, C. Canton, K. McGuinness, N. E. O’Connor, J. Torres, E. Sayrol, and X. a. Giro-i Nieto, “Salgan: Visual saliency prediction with generative adversarial networks,” in *arXiv*, January 2017.
- [24] W. Wang and J. Shen, “Deep visual attention prediction,” *IEEE Transactions on Image Processing*, vol. 27, no. 5, pp. 2368–2378, 2017.
- [25] S. Gorji and J. J. Clark, “Attentional push: A deep convolutional network for augmenting image salience with shared attention modeling in social scenes,” in *Proceedings of the IEEE Conference on Computer Vision and Pattern Recognition*, 2017, pp. 2510–2519.
- [26] X. Sun, Z. Huang, H. Yin, and H. T. Shen, “An integrated model for effective saliency prediction,” in *Proceedings of the AAAI Conference on Artificial Intelligence*, vol. 31, no. 1, 2017.
- [27] N. Liu, J. Han, D. Zhang, S. Wen, and T. Liu, “Predicting eye fixations using convolutional neural networks,” in *Proceedings of the IEEE Conference on Computer Vision and Pattern Recognition*, 2015, pp. 362–370.
- [28] J. Pan, E. Sayrol, X. Giro-i Nieto, K. McGuinness, and N. E. O’Connor, “Shallow and deep convolutional networks for saliency prediction,” in *Proceedings of the IEEE conference on computer vision and pattern recognition*, 2016, pp. 598–606.
- [29] S. Jetley, N. Murray, and E. Vig, “End-to-end saliency mapping via probability distribution prediction,” in *Proceedings of the IEEE conference on computer vision and pattern recognition*, 2016, pp. 5753–5761.
- [30] N. Liu and J. Han, “A deep spatial contextual long-term recurrent

| Setting | | Prediction method | CC | SIM | AUC Judd | NSS |
|-----------------------|-----------|------------------------|-------------------------|-------------------------|-------------------------|-------------------------|
| SETT(Gender, Other) | Cluster 1 | Clustered Universal | 0.6988 0.6368 | 0.6155 0.5624 | 0.8850 0.8772 | 2.1713 2.2750 |
| | Cluster 2 | Clustered Universal | 0.6807 0.6600 | 0.6151 0.5928 | 0.8595 0.8619 | 1.9741 2.1101 |
| | Cluster 3 | Clustered Universal | 0.6939 0.6087 | 0.6071 0.5347 | 0.8872 0.8750 | 2.2694 2.2009 |
| | Average | Clustered Universal | 0.6911 0.6352 | 0.6126 0.5633 | 0.8772 0.8714 | 2.1383 2.1953 |
| SETT(Gender, Sport) | Cluster 1 | Clustered Universal | 0.6959 0.6297 | 0.6170 0.5623 | 0.8814 0.8736 | 2.1191 2.1893 |
| | Cluster 2 | Clustered Universal | 0.6820 0.6593 | 0.6160 0.5915 | 0.8596 0.8629 | 1.9801 2.1282 |
| | Cluster 3 | Clustered Universal | 0.6980 0.6207 | 0.6075 0.5366 | 0.8925 0.8808 | 2.3202 2.3239 |
| | Average | Clustered Universal | 0.6920 0.6366 | 0.6135 0.5635 | 0.8778 0.8724 | 2.1398 2.2138 |
| SETT(Gender, Fashion) | Cluster 1 | Clustered Universal | 0.6985 0.6355 | 0.6158 0.5611 | 0.8858 0.8770 | 2.2014 2.2698 |
| | Cluster 2 | Clustered Universal | 0.6934 0.5952 | 0.6044 0.5215 | 0.8924 0.8749 | 2.3051 2.1631 |
| | Cluster 3 | Clustered Universal | 0.6810 0.6593 | 0.6155 0.5915 | 0.8610 0.8629 | 2.0036 2.1282 |
| | Average | Clustered Universal | 0.6910 0.6300 | 0.6119 0.5580 | 0.8797 0.8716 | 2.1700 2.1870 |
| SETT(Gender, Color) | Cluster 1 | Clustered Universal | 0.6948 0.6207 | 0.6054 0.5366 | 0.8916 0.8808 | 2.3423 2.3239 |
| | Cluster 2 | Clustered Universal | 0.6846 0.6593 | 0.6158 0.5915 | 0.8613 0.8629 | 2.0101 2.1282 |
| | Cluster 3 | Clustered Universal | 0.6979 0.6297 | 0.6183 0.5623 | 0.8808 0.8736 | 2.1330 2.1893 |
| | Average | Clustered Universal | 0.6924 0.6366 | 0.6132 0.5635 | 0.8779 0.8724 | 2.1618 2.2138 |
| SETT(Sport, Color) | Cluster 1 | Clustered Universal | 0.6906 0.6087 | 0.6046 0.5347 | 0.8867 0.8750 | 2.2747 2.2009 |
| | Cluster 2 | Clustered Universal | 0.6979 0.6368 | 0.6167 0.5624 | 0.8850 0.8772 | 2.1940 2.2750 |
| | Cluster 3 | Clustered Universal | 0.6809 0.6600 | 0.6121 0.5928 | 0.8574 0.8619 | 1.9753 2.1101 |
| | Average | Clustered Universal | 0.6898 0.6352 | 0.6111 0.5633 | 0.8764 0.8714 | 2.1480 2.1953 |
| SETT(Sport, Other) | Cluster 1 | Clustered Universal | 0.6976 0.6297 | 0.6179 0.5623 | 0.8835 0.8736 | 2.1329 2.1893 |
| | Cluster 2 | Clustered Universal | 0.6811 0.6600 | 0.6160 0.5928 | 0.8594 0.8619 | 1.9942 2.1101 |
| | Cluster 3 | Clustered Universal | 0.6963 0.6245 | 0.6060 0.5416 | 0.8890 0.8801 | 2.2893 2.3266 |
| | Average | Clustered Universal | 0.6917 0.6381 | 0.6133 0.5656 | 0.8773 0.8719 | 2.1388 2.2087 |

TABLE XI: Scores of ML-Net Universal saliency and ML-Net based clustered saliency, using Pix2Pix as I2I model. Each setting $SETT(f_1, \dots, f_n)$ is the setting where only features f_1, \dots, f_n with weight 0.5 were considered in clustering. "Average" in the last row of each setting is the average of the metrics for all the clusters in that setting. Higher score indicates a better performance in all metrics.

| Setting | | Prediction method | CC | SIM | AUC Judd | NSS |
|----------------------|-----------|------------------------|-------------------------|-------------------------|-------------------------|-------------------------|
| SETT(Sport, Fashion) | Cluster 1 | Clustered Universal | 0.6719 0.6479 | 0.6072 0.5851 | 0.8570 0.8596 | 1.9446 2.0866 |
| | Cluster 2 | Clustered Universal | 0.7129 0.6493 | 0.6257 0.5679 | 0.8896 0.8827 | 2.2588 2.3414 |
| | Cluster 3 | Clustered Universal | 0.6928 0.6002 | 0.6050 0.5263 | 0.8900 0.8750 | 2.2829 2.1719 |
| | Average | Clustered Universal | 0.6925 0.6325 | 0.6126 0.5598 | 0.8789 0.8724 | 2.1621 2.2000 |
| SETT(Color, Other) | Cluster 1 | Clustered Universal | 0.6858 0.6026 | 0.6029 0.5379 | 0.8796 0.8676 | 2.1343 2.1306 |
| | Cluster 2 | Clustered Universal | 0.7121 0.6493 | 0.6232 0.5679 | 0.8891 0.8827 | 2.2871 2.3414 |
| | Cluster 3 | Clustered Universal | 0.6795 0.6591 | 0.6151 0.5927 | 0.8575 0.8608 | 1.9421 2.0933 |
| | Average | Clustered Universal | 0.6925 0.6370 | 0.6137 0.5662 | 0.8754 0.8704 | 2.1212 2.1884 |
| SETT(Color, Fashion) | Cluster 1 | Clustered Universal | 0.6718 0.6476 | 0.6095 0.5857 | 0.8555 0.8584 | 1.9299 2.0666 |
| | Cluster 2 | Clustered Universal | 0.7118 0.6443 | 0.6271 0.5691 | 0.8876 0.8799 | 2.2288 2.2609 |
| | Cluster 3 | Clustered Universal | 0.6963 0.6245 | 0.6068 0.5416 | 0.8898 0.8801 | 2.3008 2.3266 |
| | Average | Clustered Universal | 0.6933 0.6388 | 0.6145 0.5655 | 0.8776 0.8728 | 2.1532 2.2180 |
| SETT(Other, Fashion) | Cluster 1 | Clustered Universal | 0.7012 0.6297 | 0.6199 0.5623 | 0.8827 0.8736 | 2.1483 2.1893 |
| | Cluster 2 | Clustered Universal | 0.6778 0.6600 | 0.6136 0.5928 | 0.8580 0.8619 | 1.9474 2.1101 |
| | Cluster 3 | Clustered Universal | 0.6969 0.6245 | 0.6070 0.5416 | 0.8898 0.8801 | 2.3219 2.3266 |
| | Average | Clustered Universal | 0.6920 0.6381 | 0.6135 0.5656 | 0.8768 0.8719 | 2.1392 2.2087 |
| SETT(Gender) | Cluster 1 | Clustered Universal | 0.6746 0.6476 | 0.6115 0.5857 | 0.8581 0.8584 | 1.9406 2.0666 |
| | Cluster 2 | Clustered Universal | 0.6996 0.6063 | 0.6083 0.5325 | 0.8874 0.8749 | 2.2719 2.1997 |
| | Cluster 3 | Clustered Universal | 0.7083 0.6469 | 0.6206 0.5660 | 0.8866 0.8821 | 2.2910 2.3302 |
| | Average | Clustered Universal | 0.6942 0.6336 | 0.6135 0.5614 | 0.8774 0.8718 | 2.1678 2.1988 |
| SETT(Color) | Cluster 1 | Clustered Universal | 0.6882 0.6600 | 0.6191 0.5928 | 0.8609 0.8619 | 2.0042 2.1101 |
| | Cluster 2 | Clustered Universal | 0.7002 0.6245 | 0.6089 0.5416 | 0.8902 0.8801 | 2.3227 2.3266 |
| | Cluster 3 | Clustered Universal | 0.6942 0.6297 | 0.6166 0.5623 | 0.8813 0.8736 | 2.1603 2.1893 |
| | Average | Clustered Universal | 0.6942 0.6381 | 0.6149 0.5656 | 0.8775 0.8719 | 2.1624 2.2087 |

TABLE XII: Continuation of Table XI.

- convolutional network for saliency detection,” *IEEE Transactions on Image Processing*, vol. 27, no. 7, pp. 3264–3274, 2018.
- [31] H. R. Tavakoli, A. Borji, J. Laaksonen, and E. Rahtu, “Exploiting inter-image similarity and ensemble of extreme learners for fixation prediction using deep features,” *Neurocomputing*, vol. 244, pp. 10–18, 2017.
- [32] S. Jia and N. D. Bruce, “Eml-net: An expandable multi-layer network for saliency prediction,” *Image and Vision Computing*, vol. 95, p. 103887, 2020.

| Setting | | Prediction method | CC | SIM | AUC Judd | NSS |
|---------------|-----------|-------------------|---------------|---------------|---------------|---------------|
| SETT(Sport) | Cluster 1 | Clustered | 0.6999 | 0.6193 | 0.8815 | 2.1488 |
| | | Universal | 0.6297 | 0.5623 | 0.8736 | 2.1893 |
| | Cluster 2 | Clustered | 0.6817 | 0.6148 | 0.8592 | 2.0060 |
| | | Universal | 0.6593 | 0.5915 | 0.8629 | 2.1282 |
| SETT(Fashion) | Cluster 1 | Clustered | 0.6947 | 0.6041 | 0.8903 | 2.3136 |
| | | Universal | 0.6207 | 0.5366 | 0.8808 | 2.3239 |
| | Cluster 2 | Clustered | 0.6921 | 0.6127 | 0.8770 | 2.1561 |
| | | Universal | 0.6366 | 0.5635 | 0.8724 | 2.2138 |
| SETT(Other) | Cluster 1 | Clustered | 0.7037 | 0.6104 | 0.8935 | 2.3125 |
| | | Universal | 0.5952 | 0.5215 | 0.8749 | 2.1631 |
| | Cluster 2 | Clustered | 0.6820 | 0.6153 | 0.8606 | 2.0110 |
| | | Universal | 0.6593 | 0.5915 | 0.8629 | 2.1282 |
| SETT(Fashion) | Cluster 1 | Clustered | 0.6967 | 0.6146 | 0.8834 | 2.2017 |
| | | Universal | 0.6355 | 0.5611 | 0.8770 | 2.2698 |
| | Cluster 2 | Clustered | 0.6941 | 0.6134 | 0.8792 | 2.1751 |
| | | Universal | 0.6300 | 0.5580 | 0.8716 | 2.1870 |
| SETT(Other) | Cluster 1 | Clustered | 0.6807 | 0.6136 | 0.8592 | 1.9848 |
| | | Universal | 0.6593 | 0.5915 | 0.8629 | 2.1282 |
| | Cluster 2 | Clustered | 0.7014 | 0.6092 | 0.8940 | 2.3165 |
| | | Universal | 0.5952 | 0.5215 | 0.8749 | 2.1631 |
| SETT(Sport) | Cluster 1 | Clustered | 0.7004 | 0.6169 | 0.8853 | 2.2188 |
| | | Universal | 0.6355 | 0.5611 | 0.8770 | 2.2698 |
| | Cluster 2 | Clustered | 0.6942 | 0.6132 | 0.8795 | 2.1734 |
| | | Universal | 0.6300 | 0.5580 | 0.8716 | 2.1870 |

TABLE XIII: Continuation of Table XII.

| Cluster | | CC | SIM | AUC Judd | NSS |
|------------|-----------|------------------------|------------------------|-----------------------|------------------------|
| Chosen | Clustered | 0.6766 ± 0.0420 | 0.5926 ± 0.0294 | 0.8739 ± 0.0274 | 2.0982 ± 0.2762 |
| | Universal | 0.646 ± 0.0449 | 0.5683 ± 0.0324 | 0.874 ± 0.0244 | 2.2264 ± 0.3052 |
| Non-chosen | Clustered | 0.6729 ± 0.0497 | 0.5941 ± 0.0329 | 0.8676 ± 0.0328 | 2.0338 ± 0.3112 |
| | Universal | 0.6401 ± 0.0480 | 0.5655 ± 0.0343 | 0.8706 ± 0.0265 | 2.1876 ± 0.3129 |

TABLE XIV: Average of scores of ML-Net Universal saliency and ML-Net based clustered saliency for assigning a new person to the chosen cluster by algorithm in III-G, where we consider personal features and all images in test set as known information of new person for assigning the person to a cluster, compared with the average of scores when assigning this person to the non-chosen clusters, for our 30 experiments. The variability of scores across 30 individuals are shown using standard deviation. Higher score indicates a better performance in all metrics.

| Cluster | | CC | SIM | AUC Judd | NSS |
|------------|-----------|------------------------|------------------------|-----------------------|------------------------|
| Chosen | Clustered | 0.6818 ± 0.0485 | 0.5994 ± 0.0291 | 0.8727 ± 0.0312 | 2.0805 ± 0.3112 |
| | Universal | 0.646 ± 0.0449 | 0.5683 ± 0.0324 | 0.874 ± 0.0244 | 2.2264 ± 0.3052 |
| Non-chosen | Clustered | 0.6694 ± 0.0451 | 0.5896 ± 0.0326 | 0.8684 ± 0.0307 | 2.0455 ± 0.2905 |
| | Universal | 0.6401 ± 0.048 | 0.5655 ± 0.0344 | 0.8706 ± 0.0265 | 2.1876 ± 0.313 |

TABLE XV: Average of scores of ML-Net Universal saliency and ML-Net based clustered saliency for assigning a new person to the chosen cluster by algorithm in III-G, where we consider only personal features as known information of new person for assigning the person to a cluster, compared with the average of scores when assigning this person to the non-chosen clusters, for our 30 experiments. The variability of scores across 30 individuals are shown using standard deviation. Higher score indicates a better performance in all metrics.

[33] M. Cornia, L. Baraldi, G. Serra, and R. Cucchiara, "Predicting human eye fixations via an lstm-based saliency attentive model," *IEEE Transactions on Image Processing*, vol. 27, no. 10, pp. 5142–5154, 2018.

[34] N. D. Bruce, C. Catton, and S. Janjic, "A deeper look at saliency: Feature

contrast, semantics, and beyond," in *Proceedings of the IEEE conference on computer vision and pattern recognition*, 2016, pp. 516–524.

[35] C. Bak, A. Kocak, E. Erdem, and A. Erdem, "Spatio-temporal saliency networks for dynamic saliency prediction," *IEEE Transactions on Mul-*

timedia, vol. 20, no. 7, pp. 1688–1698, 2017.

- [36] S. Chaabouni, J. Benois-Pineau, and C. B. Amar, “Transfer learning with deep networks for saliency prediction in natural video,” in *2016 IEEE International Conference on Image Processing (ICIP)*. IEEE, 2016, pp. 1604–1608.
- [37] S. Chaabouni, J. Benois-Pineau, O. Hadar, and C. B. Amar, “Deep learning for saliency prediction in natural video,” *arXiv preprint arXiv:1604.08010*, 2016.
- [38] L. Bazzani, H. Larochelle, and L. Torresani, “Recurrent mixture density network for spatiotemporal visual attention,” *arXiv preprint arXiv:1603.08199*, 2016.
- [39] L. Jiang, M. Xu, and Z. Wang, “Predicting video saliency with object-to-motion cnn and two-layer convolutional lstm,” *arXiv preprint arXiv:1709.06316*, 2017.
- [40] G. Leifman, D. Rudoy, T. Swedish, E. Bayro-Corrochano, and R. Raskar, “Learning gaze transitions from depth to improve video saliency estimation,” in *Proceedings of the IEEE International Conference on Computer Vision*, 2017, pp. 1698–1707.
- [41] S. Gorji and J. J. Clark, “Going from image to video saliency: Augmenting image salience with dynamic attentional push,” in *Proceedings of the IEEE Conference on Computer Vision and Pattern Recognition*, 2018, pp. 7501–7511.
- [42] W. Wang, J. Shen, F. Guo, M.-M. Cheng, and A. Borji, “Revisiting video saliency: A large-scale benchmark and a new model,” in *Proceedings of the IEEE Conference on Computer Vision and Pattern Recognition*, 2018, pp. 4894–4903.
- [43] M. Sun, Z. Zhou, Q. Hu, Z. Wang, and J. Jiang, “Sg-fcn: A motion and memory-based deep learning model for video saliency detection,” *IEEE transactions on cybernetics*, vol. 49, no. 8, pp. 2900–2911, 2018.
- [44] Y. Xu, N. Li, J. Wu, J. Yu, and S. Gao, “Beyond universal saliency: Personalized saliency prediction with multi-task cnn,” in *Proceedings of the Twenty-Sixth International Joint Conference on Artificial Intelligence, IJCAI-17*, 2017, pp. 3887–3893. [Online]. Available: <https://doi.org/10.24963/ijcai.2017/543>
- [45] Y. Xu, S. Gao, J. Wu, N. Li, and J. Yu, “Personalized saliency and its prediction,” *IEEE transactions on pattern analysis and machine intelligence*, vol. 41, no. 12, pp. 2975–2989, 2018.
- [46] B. Yu and J. J. Clark, “Personalization of saliency estimation,” *arXiv e-prints*, pp. arXiv-1711, 2017.
- [47] S. Lin and P. Hui, “Where’s your focus: Personalized attention,” *arXiv preprint arXiv:1802.07931*, 2018.
- [48] A. Li and Z. Chen, “Personalized visual saliency: Individuality affects image perception,” *IEEE Access*, vol. 6, pp. 16 099–16 109, 2018.
- [49] B. De Haas, A. L. Iakovidis, D. S. Schwarzkopf, and K. R. Gegenfurtner, “Individual differences in visual salience vary along semantic dimensions,” *Proceedings of the National Academy of Sciences*, vol. 116, no. 24, pp. 11 687–11 692, 2019.
- [50] M. Linka and B. de Haas, “Osieshort: A small stimulus set can reliably estimate individual differences in semantic salience,” *Journal of vision*, vol. 20, no. 9, pp. 13–13, 2020.
- [51] Y. Moroto, K. Maeda, T. Ogawa, and M. Haseyama, “Few-shot personalized saliency prediction based on adaptive image selection considering object and visual attention,” *Sensors*, vol. 20, no. 8, p. 2170, 2020.
- [52] T. Ishikawa and T. Yakoh, “Saliency prediction based on object recognition and gaze analysis,” *Electronics and Communications in Japan*, vol. 104, no. 2, p. e12303, 2021.
- [53] V. Badrinarayanan, A. Kendall, and R. Cipolla, “Segnet: A deep convolutional encoder-decoder architecture for image segmentation,” *IEEE transactions on pattern analysis and machine intelligence*, vol. 39, no. 12, pp. 2481–2495, 2017.
- [54] O. Russakovsky, J. Deng, H. Su, J. Krause, S. Satheesh, S. Ma, Z. Huang, A. Karpathy, A. Khosla, M. Bernstein *et al.*, “Imagenet large scale visual recognition challenge,” *International journal of computer vision*, vol. 115, no. 3, pp. 211–252, 2015.
- [55] P. Xu, K. A. Ehinger, Y. Zhang, A. Finkelstein, S. R. Kulkarni, and J. Xiao, “Turkergaze: Crowdsourcing saliency with webcam based eye tracking,” *arXiv preprint arXiv:1504.06755*, 2015.
- [56] J. Xu, M. Jiang, S. Wang, M. S. Kankanalli, and Q. Zhao, “Predicting human gaze beyond pixels,” *Journal of vision*, vol. 14, no. 1, pp. 28–28, 2014.
- [57] Y. Li, X. Hou, C. Koch, J. M. Rehg, and A. L. Yuille, “The secrets of salient object segmentation,” in *Proceedings of the IEEE conference on computer vision and pattern recognition*, 2014, pp. 280–287.
- [58] Z. Bylinskii, T. Judd, A. Oliva, A. Torralba, and F. Durand, “What do different evaluation metrics tell us about saliency models?” *IEEE transactions on pattern analysis and machine intelligence*, vol. 41, no. 3, pp. 740–757, 2018.
- [59] O. Le Meur and T. Baccino, “Methods for comparing scanpaths and saliency maps: strengths and weaknesses,” *Behavior research methods*, vol. 45, no. 1, pp. 251–266, 2013.
- [60] R. J. Peters, A. Iyer, L. Itti, and C. Koch, “Components of bottom-up gaze allocation in natural images,” *Vision research*, vol. 45, no. 18, pp. 2397–2416, 2005.
- [61] A. Lancichinetti and S. Fortunato, “Community detection algorithms: A comparative analysis,” *Phys. Rev. E*, vol. 80, p. 056117, Nov 2009. [Online]. Available: <https://link.aps.org/doi/10.1103/PhysRevE.80.056117>
- [62] V. D. Blondel, J.-L. Guillaume, R. Lambiotte, and E. Lefebvre, “Fast unfolding of communities in large networks,” *Journal of statistical mechanics: theory and experiment*, vol. 2008, no. 10, p. P10008, 2008.
- [63] M.-Y. Liu, T. Breuel, and J. Kautz, “Unsupervised image-to-image translation networks,” *arXiv preprint arXiv:1703.00848*, 2017.
- [64] P. Isola, J.-Y. Zhu, T. Zhou, and A. A. Efros, “Image-to-image translation with conditional adversarial networks,” in *Proceedings of the IEEE conference on computer vision and pattern recognition*, 2017, pp. 1125–1134.
- [65] O. Ronneberger, P. Fischer, and T. Brox, “U-net: Convolutional networks for biomedical image segmentation,” in *Medical Image Computing and Computer-Assisted Intervention – MICCAI 2015*, N. Navab, J. Hornegger, W. M. Wells, and A. F. Frangi, Eds. Cham: Springer International Publishing, 2015, pp. 234–241.